

1 **AA Central Asia Hydrologic Monitoring Dataset for Food and**  
2 **Water Security Applications in Central AsiaAfghanistan,**

3 Amy L. McNally<sup>1,2,3</sup>, Jossy Jacob<sup>1,4</sup>, Kristi Arsenault<sup>1,2</sup>, Kimberly Slinski<sup>1,5</sup>, Daniel P. Sarmiento<sup>1,2</sup>,  
4 Andrew Hoell<sup>6</sup>, Shahriar Pervez<sup>7</sup>, James Rowland<sup>8</sup>, Mike Budde<sup>8</sup>, Sujay Kumar<sup>1</sup>, Christa Peters-  
5 Lidard<sup>1</sup>, James P. Verdin<sup>3</sup>

6  
7 1 NASA Goddard Space Flight Center, Greenbelt, MD, 20771, United States

8 2 ~~SAIC~~, Science Applications International Corporation Inc., Reston, VA, 20190, United States

9 3 ~~United States~~U.S. Agency for International Development, Washington, DC, 20523, United States

10 4 ~~SSAI~~Science Systems and Applications Inc., Lanham, MD, ~~postal code~~20706, United States

11 5 University of Maryland Earth Systems Science Interdisciplinary Center, College Park, MD,  
12 20740, United States

13 6 National Oceanic and Atmospheric Administration, Physical Science Laboratory, Boulder, CO,  
14 80305, United States

15 7 Arctic Slope Regional Corporation (~~ASRC~~) Federal Data Solutions, Contractor to U.S. Geological  
16 Survey, Earth Resources Observation and Science (EROS) Center (~~EROS~~), Sioux Falls, SD, 57198,  
17 United States

18 8 ~~United States~~U.S. Geological Survey, EROS Center, Sioux Falls, South Dakota, 57198, United  
19 States

21 Correspondence to: Amy L. McNally (amy.l.mcnally@nasa.gov)

Style Definition: Normal (Web)

Formatted: Font color: Auto

Formatted: Font color: Auto

Formatted: Font color: Auto

Formatted: Font color: Auto

Formatted: Font color: Auto

Formatted: Font color: Auto

Formatted: Font color: Auto

Formatted: Font color: Auto

## Abstract

From the Hindu Kush Mountains to the Registan desert, Afghanistan is a diverse landscape where droughts, floods, conflict, and economic market accessibility pose challenges for agricultural livelihoods and food security. The ability to remotely monitor environmental conditions is critical to support decision making for humanitarian assistance. The [Famine Early Warning Systems Network \(FEWS NET\)](#) Land Data Assimilation System (FLDAS) global and Central Asia data streams [described here combine meteorological reanalysis datasets and land surface models to generate provide information on hydrologic states for routine integrated food security analysis. While developed for a specific project, these data are publicly available and useful for other applications that require hydrologic estimates of snow-covered fraction, snow water equivalent, soil moisture, runoff and other variables representing the water and energy balance. This approach allows us to fill the gap created by the lack of in situ hydrologic data in the region. First, we describe the configuration of the FLDAS and the These two resultant data streams: one, are unique because of their suitability for routine monitoring, as well as a historical record for computing relative indicators of water availability. The global, stream is available at ~1 month latency, provides monthly average outputs on a 10-km<sup>2</sup>-km grid from 1982-present. The second data stream, Central Asia, \(30-100 °E, 21-56 °N\), at ~1 day latency, provides daily average outputs on a 1-km<sup>2</sup> grid from 2001-present. We describe our verification of these data that are compared to other remotely sensed estimates as well as qualitative field reports. These -km grid from 2000-present. This paper describes the configuration of the two FLDAS data streams, background on the software modeling framework, selected meteorological inputs and parameters, and results from previous evaluation studies. We also provide additional analysis of precipitation and snow cover over Afghanistan. We conclude with an example of how these data and value-added products \(e.g., anomalies and interactive time-series\) are used in integrated food security analysis. These data are hosted by the National Aeronautics and Space Administration \(NASA\) and USGS U.S. Geological Survey data portals for public use. The global data stream with a longer record, is useful for exploring interannual variability, relationships with atmospheric-oceanic teleconnections \(e.g., ENSO\), trends over time, and monitoring drought. Meanwhile, the higher spatial resolution Central Asia data stream, with lower latency, is useful for simulating snow-hydrologic dynamics in complex topography for monitoring snowpack and flood risk. use in new and innovative studies that will improve understanding of this region.](#)

## 1 Introduction

[From the Hindu Kush Mountains to the Registan desert, Afghanistan is a diverse landscape where droughts, floods, conflict, and economic market accessibility pose challenges for agricultural livelihoods and food security. The ability to remotely monitor environmental conditions is critical to support decision making for economic development, humanitarian assistance, water resource management, agriculture and more. Environmental datasets can be combined with socio-economic](#)

Formatted: Font color: Auto

61 variables and transformed into customized products to support decision making. This is the  
62 definition of a ‘climate service’ (Hewitt et al., 2012).

63  
64 Hydrologic and land surface datasets are particularly relevant for agriculture and water resources  
65 decision making. When these datasets are credible, updated routinely, and made publicly available,  
66 the influences of climate variability and climate change can be incorporated into specialized  
67 analyses by intermediary users<sup>1</sup>. One example of an intermediary user central to this data descriptor  
68 is the food security analysts of the Famine Early Warning Systems Network (FEWS NET). FEWS  
69 NET analysts combine environmental information, largely from remote sensing and earth system  
70 models, with information on nutrition, livelihoods, markets, and trade to provide decision support to  
71 the U.S. Agency for International Development (USAID) Bureau of Humanitarian Assistance.  
72 Additional examples and discussion of the production of climate service inputs can be found in the  
73 literature (e.g., Vincent et al., 2018; McNally et al., 2019).

74  
75 While these data are tailored to specific needs, they are also applicable to other climate services and  
76 research e.g., Desert Locusts movement forecasting (Tabar et al., 2021). To that end, this paper  
77 describes the FEWS NET Land Data Assimilation System (FLDAS) global and Central Asia data  
78 streams. The inputs (e.g., precipitation) and resulting hydrologic estimates (a) provide a 40+ year  
79 historical record for contextualizing estimates in terms of departures from average (i.e., anomalies),  
80 (b) are low latency (< 1-month) for timely decision support, and (c) are familiar to the food and  
81 water security user-community.

82  
83 The purpose of this data descriptor is four-fold:

- 84 • to describe the development of the moderate resolution, low latency FLDAS hydrologic  
85 monitoring system for Central Asia, specifically Afghanistan
- 86 • to increase awareness of these data resources, which are intended to be a public good,  
87 to demonstrate how our methods inform critical investigations that ultimately improve  
88 general understanding of water resources in this important region of the world, and
- 89 • to describe a ‘convergence of evidence’ approach to hydrologic monitoring in locations  
90 where all sources of information contain some level of uncertainty.

91  
92 An outline of this data descriptor is as follows. 1.1 Central Asia Weather and Climate Section 1.1  
93 provides background on Afghanistan Weather and Climate. Section 1.2 reviews previous studies  
94 that have conducted evaluations of the meteorological inputs and hydrologic outputs of Land Data  
95 Assimilation Systems in the Central Asia region. Section 2 (Methods) describes the hydrologic  
96 modeling system, parameters and meteorological inputs, and model outputs. Section 3 (Results)  
97 presents comparisons of precipitation inputs, and comparisons of modeled snow estimates to  
98 remotely sensed snow observations. Finally, Section 4 describes an application of these data to the  
99 Afghanistan drought of 2018.

---

<sup>1</sup>The WMO defines intermediate (intermediary) users as those who transform climate information into a climate service

1.1 Afghanistan Weather and Climate

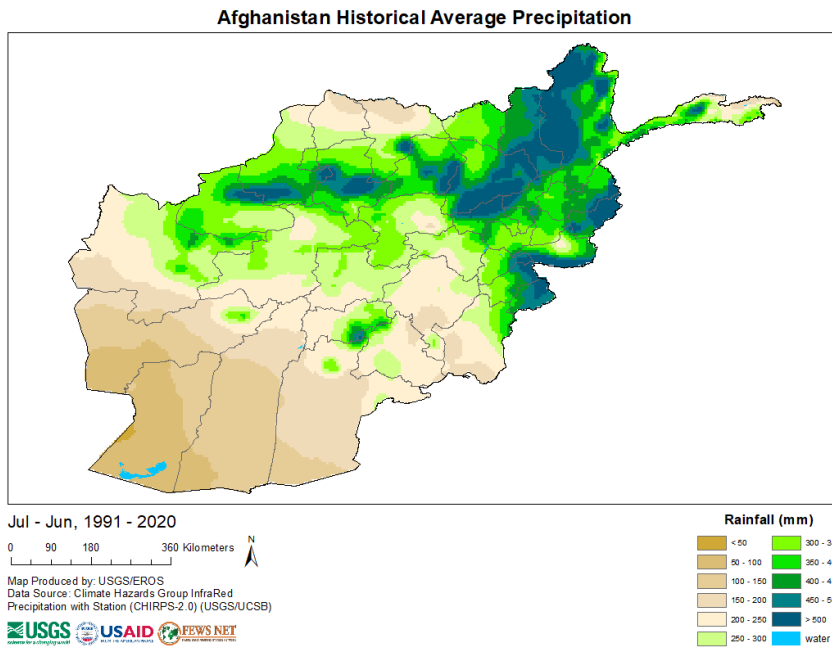


Figure 1a. Mean annual precipitation in Afghanistan from 1991-2020, overlaid on province boundaries. Map (USGS Knowledge Base, 2021) with data from Funk et al. (2015).

Formatted: Normal

Afghanistan Historical Average Maximum Temperature

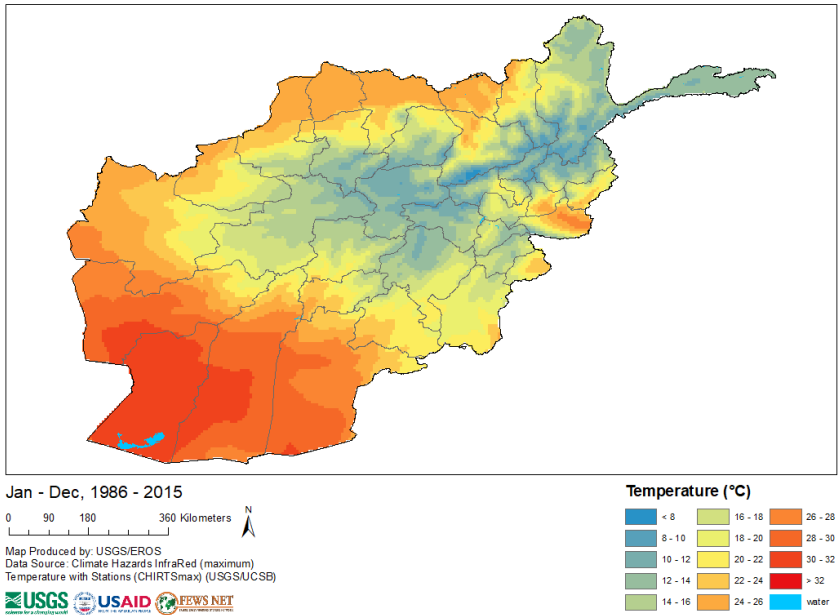


Figure 1b. Average maximum monthly temperature from (1986-2015), overlaid on province boundaries. Map (USGS Knowledge Base, 2021) with data from Verdin et al. (2020).

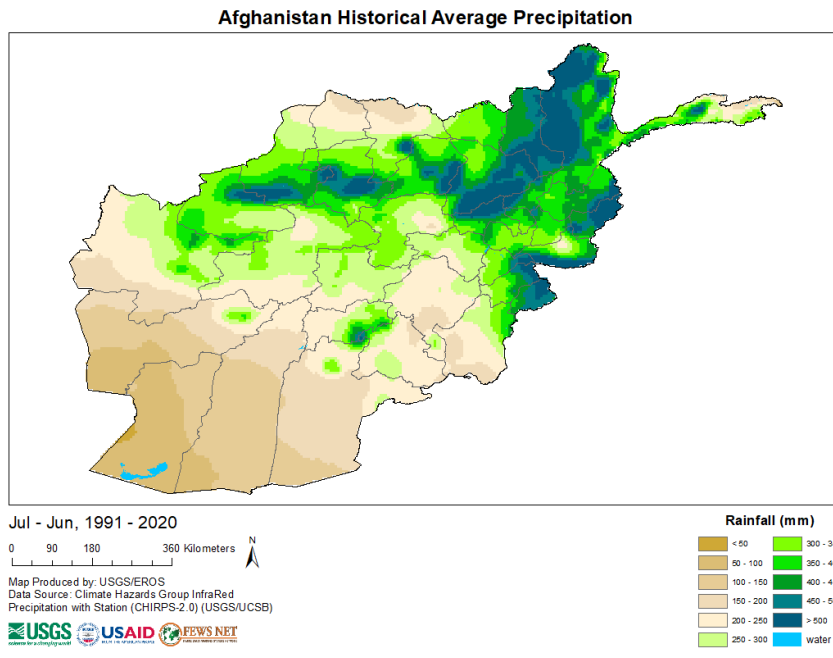
Central Asia, a region that includes Afghanistan, is water-scarce, receiving roughly 75% of its annual precipitation during November–April (Oki and Kanai, 2006). In Afghanistan, rainfall is highest in the northeast Hindu Kush Mountains and decreases toward the arid southwest Registan Desert (Fig. 1a). Temperature follows a similar pattern with cooler temperatures in the high elevation and, wetter northeast and warmer temperatures in the south and southwest (Fig. 1b). Regional precipitation is strongly influenced by the El Niño–Southern Oscillation (ENSO). La Niña conditions are associated with below average precipitation (FEWS NET, 2020b) and El Niño conditions associated with above average precipitation (Barlow et al., 2016; Hoell et al., 2017; Rana et al., 2018; Hoell et al., 2018, 2020; FEWS NET, 2020a) are associated with above average precipitation (Barlow et al., 2016; Hoell et al., 2017; Rana et al., 2018; Hoell et al., 2018, 2020; FEWS NET, 2020a). Other dynamical factors with an important influence on precipitation include orography, storm tracks, and the Madden–Julian oscillation (MJO) (Barlow et al., 2005; Nazemosadat and Ghaedamini, 2010; Hoell et al.,

Formatted: Font color: Auto

Formatted: Font color: Auto

Formatted: Font color: Auto

122 2018). (Barlow et al., 2005; Nazemosadat and Ghaedamini, 2010; Hoell et al., 2018). The last  
123 several years have experienced a number of several ENSO events, with recent La Niña events in  
124 2016-17, 2017-18, and 2020-2021+2022 (NOAA CPC ENSO Cold & Warm Episodes by Season,  
125 2021) that corresponded to droughts (FEWS NET, 2017b, 2018c, 2021).  
126



127  
128 Figure 1a. Average annual precipitation in Afghanistan from 1991-2020, with overlaid province  
129 boundaries. Map source (USGS Knowledge Base, 2021).

Formatted: Font color: Auto

Formatted: Normal

Afghanistan Historical Average Maximum Temperature

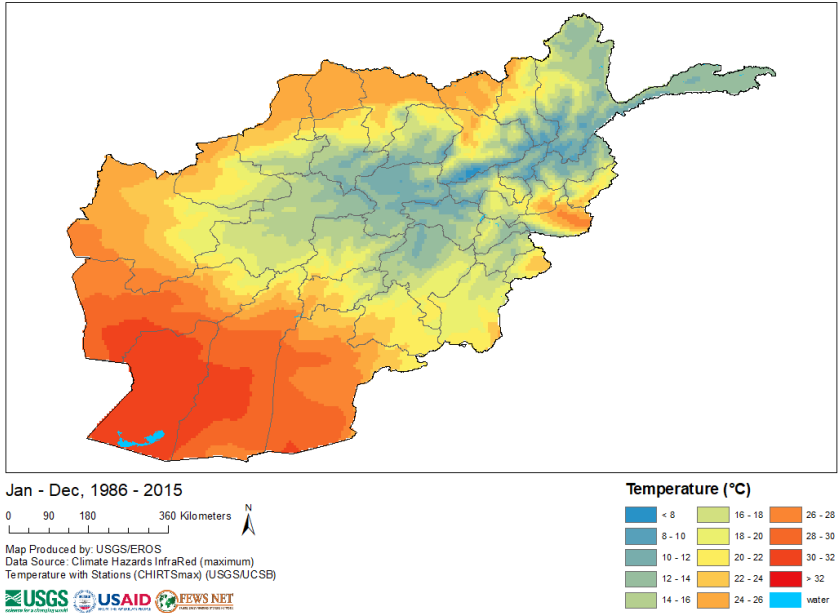


Figure 1b. Average maximum monthly temperature from (1986-2015), overlaid with province boundaries. Map source (USGS Knowledge Base, 2021).

Despite Afghanistan's semi-arid climate, agriculture is an important sector, contributing 23% of the its gross domestic product and employing 44% of the national labor force (CIA World Factbook). High mountain snowpack and snowmelt runoff are important for agricultural water supply, and according to the Famine Early Warning Systems Network (FEWS NET, 2018b). According to FEWS NET (2018b) snowmelt runoff is responsible for "providing over 80% of irrigation water used. The timing and duration of the snowmelt is a key factor in determining the volume of irrigation water and the length of time that it is available, as well as its availability for use in marginal areas that experience [variable] rainfall." Therefore, routine hydrologic monitoring, with particular emphasis on snow, is critical for tracking agricultural conditions and provides early warning for food insecurity.

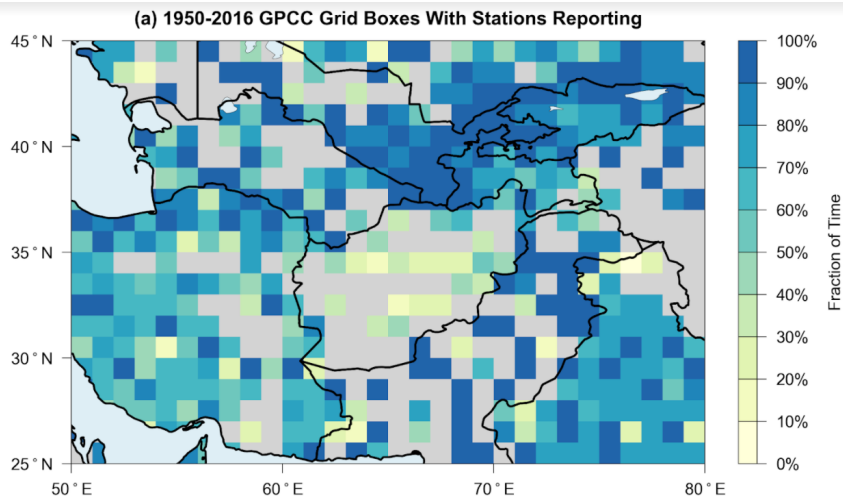
## 1.2 Precipitation Hydrologic Data Availability and Uncertainty

Remote sensing and models are important inputs to climate services (Qamer et al., 2019). In the Central Asia region, and especially Afghanistan estimates of meteorological inputs, and model parameters have considerable uncertainty due to sparse in situ environmental observations. To address these challenges, the NASA High Mountain Asia project (<https://www.himat.org/>) has broadly aimed to explore the driving changes in hydrology as well as model validation and data assimilation, and water budget processes from the Himalayas in the south and east to the Hindu Kush in the west. These efforts and other studies of satellite derived rainfall informed the configuration and interpretation of the FLDAS Central Asia and global data streams. Sparse in-situ precipitation observations lead to uncertainty in gridded and satellite-based precipitation estimates which are important for environmental monitoring and driving hydrologic models. Precipitation station observations are used for (a) bias correction of satellite estimates and (b) validation of gridded products. In terms of gridded dataset development, Hoell et al. (2015) describe lack of station observations in Afghanistan, Iraq and Pakistan and how complex topography in these locations makes this issue particularly problematic. Barlow et al. (2016) also highlight the station availability across the region and how that influences uncertainties in the Global Precipitation Climatology Center (GPCC) version 6 dataset over Central Asia (Fig. 2a) and specifically Afghanistan over time (Fig. 2b). Related to validation, Yoon et al. (2019) highlight that the representativeness of the sparse in-situ data is a serious limitation in their evaluation of precipitation over High Mountain Asia.

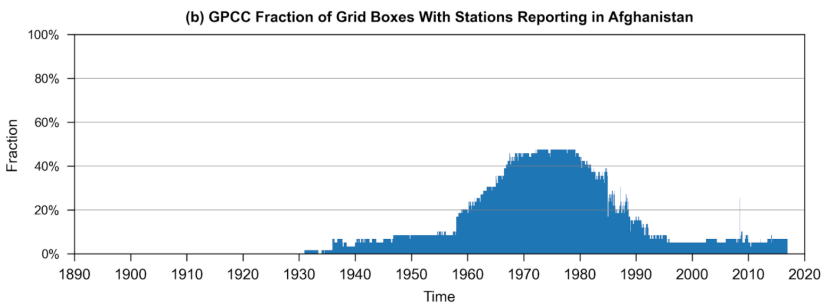
The primary challenge to producing and evaluating hydrologic estimates is that sparse in situ precipitation observations lead to uncertainty in gridded, satellite-based precipitation estimates. Precipitation station observations are used for (a) bias correction of satellite estimates and (b) validation of gridded products. In terms of gridded dataset development, Hoell et al. (2015) describe how lack of station observations and complex topography in Afghanistan, Iraq, and Pakistan makes this issue particularly problematic. Barlow et al. (2016) also highlight the station availability across the region and how that influences uncertainties in the Global Precipitation Climatology Center (GPCC) version 6 (Schneider et al., 2017) dataset over Central Asia (Fig. 2a) and specifically Afghanistan over time (Fig. 2b).

Formatted: Normal





175



176

177

178

179

180

181

182

183

184

185

Figure 2. (a) Station data availability underlying the GPCC version 6 dataset, for the 1951–2016 period, on the 0.5°-resolution grid over Central Asia. (b) Fraction of gridcells with Stations used as input to the GPCC rainfall dataset in Afghanistan from 1932–2016.

In the absence of abundant in situ observations, one approach for remote sensing and model evaluation is to compare multiple input datasets and evaluate the water balance. Independent observations from the different components of the water balance (e.g., evapotranspiration, soil moisture, streamflow) help constrain estimates. We provide some background here and refer readers

186 and data users to literature from the NASA High Mountain Asia project, specifically Yoon et al.  
187 (2019) and Ghatak et al. (2018), who explored similar configurations to the FLDAS system. This  
188 background allows the reader to appreciate the uncertainties in inputs, outputs and derived products  
189 and climate services over Afghanistan and the broader Central Asia region.

190  
191 Meteorological forcing is known to be the primary source of uncertainty in land surface model  
192 simulations (Kato and Rodell, 2007). Thus, its evaluation is important to understand the quality of  
193 model inputs and outputs. For this reason, Ghatak et al. (2018) compare four unique precipitation  
194 data sources: daily Climate Hazards center Infrared Precipitation with Stations (CHIRPS) (Funk et  
195 al., 2015), NOAA’s Global Data Assimilation System (GDAS) (Derber et al., 1991), and two  
196 estimates from NASA’s Modern Era Reanalysis for Research and Applications version 2 (MERRA-  
197 2) (Gelaro et al., 2017). They find that annual CHIRPS and GDAS precipitation estimates had  
198 similar bias and root mean squared error over Afghanistan with respect to APHRODITE (Asian  
199 Precipitation Highly Resolved Observational Data Integration Toward Evaluation) rain-gauge  
200 derived product (Yatagai et al., 2012). CHIRPS had a higher correlation with APHRODITE. Ghatak  
201 et al. (2018) further evaluated the quality of rainfall inputs based on the performance of  
202 evapotranspiration and other derived outputs. The authors caution that gridded precipitation  
203 estimates that have in situ inputs, like CHIRPS, may systematically underestimate precipitation in  
204 mountainous regions. We keep this consideration in mind when interpreting differences between  
205 FLDAS global and Central Asia data streams.

206  
207 Yoon et al. (2019) compare precipitation estimates from 10 different products including  
208 APHRODITE, CHIRPS, GDAS, and MERRA-2, across a broad region of High Asia, including a  
209 portion of Afghanistan. They find that all datasets generally capture the spatial pattern of rainfall  
210 and that the products tend to agree more at high elevations, where it is unlikely there are station  
211 observations. Like Ghatak et al. (2018), they found CHIRPS and APHRODITE to have a lower  
212 average precipitation than GDAS, attributable to the incorporation of sparse gauge data.

213  
214 In addition to precipitation, other meteorological inputs are important for accurate hydrologic  
215 estimates. Yoon et al. (2019) conducted an intercomparison of near surface air temperature  
216 estimates from three model analysis products (European Centre for Medium-Range Weather  
217 Forecasts (ECMWF; Molteni et al., 1996), GDAS, and MERRA-2). They noted a statistically  
218 significant upward trends in GDAS and ECMWF temperature, as well as consistently higher  
219 temperatures in MERRA-2. We see the same pattern when averaging across Afghanistan. Yoon et  
220 al. (2019) conclude that improvements in the meteorological boundary conditions would be needed  
221 to reduce the uncertainty in the terrestrial budget estimates. These sentiments are echoed in Qamer  
222 et al. (2019).

223  
224 Despite known uncertainties, Schiemann et al. (2008)(2008) find that gridded precipitation estimates  
225 can qualitatively identify large scale spatial distribution of precipitation, seasonal ~~eye~~cycles, and  
226 interannual variability (i.e., wet and dry years) across Central Asia. Long-term estimates of rainfall  
227 from satellite derived products, as well as derived ~~historie~~historical time series from hydrologic

Formatted: Font: +Body (Times New Roman)

Formatted: Font: Not Italic

228 modelling~~modeling~~, can be used as a baseline of “observations,” from which we can have a sense of  
229 relative conditions, i.e., anomalies and variability. When this historical record is harmonized with a  
230 routine monitoring system, current conditions can be placed in historical context. Anomaly-based  
231 representation of hydrologic extremes can provide confidence in modeled estimates that have the  
232 potential to influence agricultural, water resources and food security outcomes. For these reasons  
233 one of the requirements for FLDAS input is that there is a sufficiently long historical record for  
234 contextualizing estimates in terms of anomalies.

235  
236 In addition to reliance on the representation of relatively wet and dry conditions, a “convergence of  
237 evidence” approach that draws on (quasi-)independent sources of information is useful to  
238 understand actual conditions. For convergence of Earth observations, hydrologic models can  
239 generate ensembles of historic, current or future estimates of snow, streamflow, soil moisture, and  
240 evapotranspiration which can then be compared to satellite derived estimates of surface water (e.g.  
241 McNally et al., 2019), soil moisture (e.g. McNally et al., 2016), vegetation conditions and  
242 evapotranspiration (e.g. Pervez et al., 2021; Jung et al., 2019), snow cover (e.g. Arsenault et al.,  
243 2014), in situ stream flow. From a climate services perspective, the reliance on the representation of  
244 relatively wet and dry conditions, as well as a “convergence of evidence” approach, provide useable  
245 information despite the above-mentioned uncertainties. A convergence of evidence approach that  
246 draws on (quasi-) independent sources of information is useful to understand actual conditions. For  
247 convergence of Earth observations, hydrologic models can generate ensembles of historical, current,  
248 or future estimates of snow, streamflow, soil moisture, and evapotranspiration, which can then be  
249 compared to satellite derived estimates of surface water (e.g., McNally et al., 2019), soil moisture  
250 (e.g., McNally et al., 2016), vegetation conditions and evapotranspiration (e.g., Jung et al., 2019;  
251 Pervez et al., 2021), snow cover (e.g., Arsenault et al., 2014), in situ streamflow (e.g. Jung et al.,  
252 2017) and others. Hydrologic estimates can also be compared to outcomes in crop production e.g.  
253 (McNally et al., 2015; Davenport et al., 2019; Shukla et al., 2020), and nutrition, health, and food  
254 security (e.g. Grace and Davenport, 2021) to provide a qualitative understanding of both hydrologic  
255 model performance and conditions on the ground. In this paper we provide an example of 2018  
256 where drought conditions were associated with crisis levels of acute food insecurity over most of  
257 Afghanistan and others. Hydrologic estimates can also be compared to outcomes in crop production  
258 (e.g., (e.g., McNally et al., 2015; Davenport et al., 2019; Shukla et al., 2020), and nutrition, health,  
259 and food security (e.g., Grace and Davenport, 2021) to provide a qualitative understanding of both  
260 hydrologic model performance and conditions on the ground. In this paper we provide an example  
261 for 2018 where drought conditions were associated with crisis levels of acute food insecurity over  
262 most of Afghanistan (FEWS NET, 2018c).

263  
264 This paper describes the FLDAS hydrologic modeling system’s global and Central Asia data  
265 streams, which are designed for food and water security applications. These data streams provide a  
266 long historic record for contextualizing estimates, as well as low latency data for timely decision  
267 support. These data streams can also support research and monitoring by the broader food and water  
268 security community. To summarize, our experience and the literature have characterized  
269 uncertainties in available meteorological forcing for the region. GDAS, CHIRPS, and MERRA-2

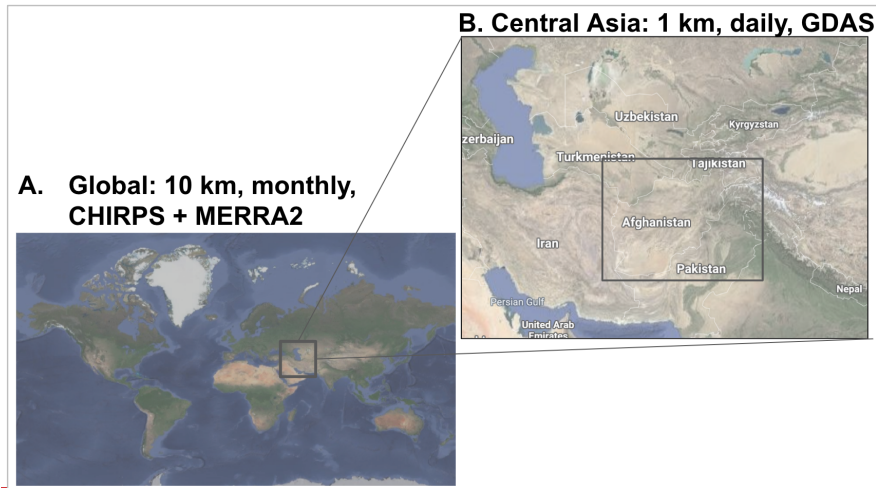
Formatted: Font: +Body (Times New Roman)

Formatted: Font: +Body (Times New Roman)

Formatted: Font: +Body (Times New Roman)

270 were chosen for the FLDAS system based on our project requirements of (a) a sufficiently long  
271 historical record for contextualizing estimates in terms of anomalies (b) low latency (< 1-month) for  
272 timely decision support, (c) familiar to the FEWS NET user-community, and (d) prior evaluation by  
273 our team and the broader community. We note here and describe in more detail later that the  
274 Integrated Multi-satellite Retrievals for the Global Precipitation Mission (IMERG), a NASA  
275 precipitation product (Huffman et al., 2020) also meets these requirements, since version 6 which  
276 was released in 2019 (after these studies and initial FLDAS configuration). We will describe  
277 IMERG, GDAS, and MERRA-2 comparison in the Results (Section 3).  
278 ~~The purpose of this data descriptor is four fold: (1) describe the development of the moderate~~  
279 ~~resolution, low latency FLDAS system to inform hydrologic monitoring for Central Asia,~~  
280 ~~specifically Afghanistan, (2) increase awareness of these data resources which are intended to be a~~  
281 ~~public good, (3) demonstrate how our methods inform critical investigations that ultimately~~  
282 ~~improve general understanding of water resources in this important region of the world, and (4)~~  
283 ~~advocate for a convergence of evidence approach to hydrologic monitoring in locations where all~~  
284 ~~sources of information contain some level of uncertainty. An outline of this data descriptor is as~~  
285 ~~follows.~~ First, in the Methods (section 2) we describe the hydrologic modeling system, parameters  
286 and meteorological inputs and model outputs. In the Results (section 3) we report comparisons to  
287 other precipitation estimates, as well as comparisons of modeled snow estimates to remotely sensed  
288 snow observations and find generally good agreement. Finally, we describe an application (section  
289 4) of these data to the Afghanistan drought of 2018.

## 290 2 Methods



291 **Figure 3.** The FEWS NET Land Data Assimilation System (FLDAS) domains for (A) the global  
292 data stream at 10 km<sup>2</sup> spatial resolution, and ~1 month latency for monthly averaged hydrologic  
294 estimates and (B) the Central Asia data stream at 1 km<sup>2</sup> spatial resolution and ~1 day  
295 latency for daily averaged hydrologic estimates.

### 296 2.1 Land Surface Modeling System & Parameters

297 Land surface models (LSMs model (LSM) can provide spatially and temporally continuous  
298 information about the water and energy budgets of the land surface. This information is useful for  
299 food and water security applications in places where in situ measurements of rainfall, soil moisture,  
300 snow and runoff are sparse. This is particularly relevant in mountainous places like Afghanistan  
301 where heterogeneous geography limits the representativeness of sparse in situ measurements. We  
302 use NASA's Land Information System Framework (LISF), which is comprised of a pre-processor,  
303 the Land Data Toolkit (Arsenault et al., 2018) The FLDAS (McNally et al., 2017) utilizes the  
304 NASA's Land Information System Framework (LISF), which is composed of a pre-processor, the  
305 Land surface Data Toolkit (Arsenault et al., 2018), the Land Information System (Kumar et al.,  
306 2006; Peters-Lidard et al., 2007), and the Land Verification Toolkit (Kumar et al., 2012). To support  
307 the needs of FEWS NET we have developed a custom instance of the NASA LISF – the FEWS NET  
308 Land Data Assimilation System (FLDAS) (McNally et al., 2017). In this data descriptor we describe  
309 the two configurations of the FLDAS data streams used for Central Asia food and water security  
310 applications. In this data descriptor we describe the two configurations of the FLDAS data streams

Formatted: Font color: Auto

Formatted: Font color: Auto

β11 used for Central Asia food and water security applications. It uses the Noah 3.6 Land Surface  
β12 Model LSM (Chen et al., 1996; Ek et al., 2003)(Chen et al., 1996; Ek et al., 2003) and has for the  
β13 two data streams. One, (Fig. 3 and Table 1). The first data stream is global, at ~1 month latency, and  
β14 provides monthly average outputs on a 10-km<sup>2</sup>-km grid from 1982-present. The second data stream,  
β15 centered on Central Asia, ~1 day latency, provides daily average outputs at 1-km<sup>2</sup>-km from 2001-  
β16 present.

β17  
β18 One important feature, added by the NASA LISF software development team, is the radiation  
β19 correction described in Kumar et al. (2013), which improves the representation of snow dynamics  
β20 with respect to slope and aspect corrections on the downward solar radiation field. Another  
β21 noteworthy feature is the method of the Central Asia data stream restart (i.e., annual initialization  
β22 based on climatology), which was developed to address an issue of excessive inter-annual snow  
β23 accumulation found in the Noah LSM. First, a nine-year spin-up of the system was performed to  
β24 produce stable snow and soil moisture conditions. Next, the resulting model states were compared  
β25 with the Moderate Resolution Imaging Spectroradiometer (MODIS) Maximum Snow Extent data  
β26 originally computed by NOAA National Operational Hydrologic Remote Sensing Center (Greg Fall,  
β27 NOAA Operational Data Center, written communication., 2014) . Then, the model-estimated  
β28 conditions were adjusted to produce a climatological model state for 1 October that is used to  
β29 initialize each year. This approach ensures that the ‘water year,’ beginning 1 October, is initialized  
β30 with a reasonable initial amount of snowpack. While this method does effectively manage excessive  
β31 inter-annual modeled snow accumulation, the user should be aware that using the climatological  
β32 model state will persist for ~1-2 months in the water and energy balance of the LSM until they are  
β33 superseded by “observed” meteorological inputs for the current water year. Preliminary work  
β34 indicates that this issue will be resolved in future updates. In contrast, the global data stream does  
β35 not use this 1 October initialization procedure.  
β36 Although the two data stream specifications are largely the same, there are some differences related  
β37 to the input forcings, parameters and specifications (Table 1) and also model spin-up  
β38 procedure procedures.  
β39

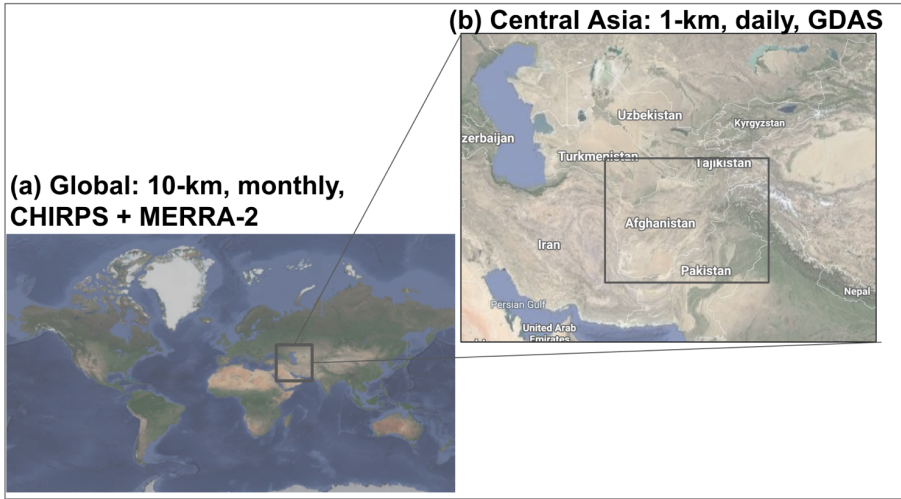


Figure 3. The FEWS NET Land Data Assimilation System (FLDAS) domains for (a) the global data stream at 10-km spatial resolution and ~1 month latency for monthly averaged hydrologic estimates and (b) the Central Asia data stream at 1-km spatial resolution and ~1 day latency for daily averaged hydrologic estimates.

Table 1. FEWS NET Land Data Assimilation System (FLDAS) specifications for (A) global data stream, 10-km<sup>2</sup>-km monthly with CHIRPS+MERRA-2; and (B) Central Asia data stream, 1-km<sup>2</sup>-km, daily with GDAS.

	Global	Central Asia
Spatial Extent	179.95°W- 179.95°E, 59.95°S- 89.95°N	30-100°E, 21-56°N
Landmask	Land Data Toolkit (LDT) generated from MODIS (Arsenault et al. 2018) using LISF-LDT, with MOD44w mask applied post-processing.	MOD44w (Carroll et al., 2017) MOD44w (Carroll et al., 2017)
Landcover	IGBP landcover	IGBP landcover
Parameters	FAO Soils Reynolds et al (2000)	FAO Soils

Formatted Table

Elevation	<a href="#">Shuttle Radar Topography Mission SRTM (NASA JPL, 2013)</a>	SRTM
Albedo	<a href="#">NCEP albedo (Csiszar, I., and Gutman 1999)</a>	NCEP albedo
Albedo	<a href="#">Native Max Snow Albedo; Barlage (2005); National Centers for Environmental Prediction (NCEP) albedo (Csiszar and Gutman, 1999) &amp; MODIS-based Max Snow Albedo (Barlage et al., 2005)</a>	Native NCEP albedo & MODIS-based Max Snow Albedo
Vegetation Parameters	<a href="#">NCEP greenness fraction (Gutman and Ignatov 1997)</a> <a href="#">NCEP greenness fraction (Gutman and Ignatov, 1998)</a>	NCEP greenness fraction
Non-Precipitation Meteorological Inputs	<a href="#">MERRA-2 meteorological variables</a>	GDAS <a href="#">meteorological variables</a>
Soil Texture	<a href="#">FAO STATSGO soil texture</a> <a href="#">Food and Agricultural Organization (FAO) soil texture &amp; properties (Reynolds et al., 2000)</a>	FAO STATSGO soil texture & properties
Precipitation Inputs	CHIRPS daily precipitation, downscaled to <a href="#">36-hourly</a> with LDT	GDAS 3-hourly precipitation
Specifications	Noah 3.6.1	Noah 3.6.1
Map Projection	Geographic Latitude-Longitude	Geographic Latitude-Longitude
Software Version	7.2	7.3
Spatial Resolution	<a href="#">0.1-degree</a> <a href="#">10-km</a>	<a href="#">0.01-degree</a> <a href="#">1-km</a>
Temporal Coverage	1982-01-01 to present	<del>2004</del> <a href="#">2000</a> -10-01 to present
Model Timestep	<del>30</del> <a href="#">15</a> -min timestep	<del>15</del> <a href="#">30</a> -min timestep
Met. Forcing Heights	<del>2m</del> <a href="#">2-m</a> Air Temperature (Tair), <del>10m</del> <a href="#">10-m</a> Wind	<del>2m</del> <a href="#">2-m</a> Tair, <del>10m</del> <a href="#">10-m</a> Wind
Soil layers (meters)	0-0.1; 0.1-0.4; 0.4-1.0; 1-2	0-0.1; 0.1-0.4; 0.4-1.0; 1-2
Features	radiation correction	radiation correction

Formatted Table

Formatted Table

Formatted Table

Formatted: Font: +Body (Times New Roman)

349

350 The parameters and specifications listed in Table 1 are largely default settings defined by the Noah  
 351 LSM community (NCAR Research Applications Library, 2021). [Ongoing research aims to identify](#)



352 where model output performance can be improved with parameter updates. Evaluating parameter  
353 updates had similar challenges as evaluating input forcing described in Section 1.2: without reliable  
354 reference data it is difficult to determine a “best” input. For example, we have explored changing  
355 soil parameters from FAO to International Soil Reference and Information Centre (ISRIC) SoilGrids  
356 database (Hengl et al., 2017). This change did not result in improvements in streamflow statistics in  
357 southern Africa, nor in soil moisture anomalies’ ability to represent drought events. We expect  
358 similar results in Afghanistan where, e.g., streamflow will be sensitive to a change in soil  
359 parameters and the lack of referenced data to evaluate if there is an improvement. Moreover, our  
360 model runs at 0.1 and 0.01 degrees may not fully exploit the added value of the 250m soil grids as  
361 noted in Ellenburg et al. (2021) for a LISF application in East Africa.

362 Vegetation parameters are also potential sources of improvement whose importance to LDAS  
363 hydrologic estimates has been highlighted (e.g., Miller et al., 2006). We have found the NCEP  
364 estimates of green vegetation fraction (GVF) to be sufficient for this configuration of Noah 3.6. We  
365 found that a time series of GVF derived from the Normalized Difference Vegetation Index (NDVI)  
366 did not improve representation of droughts in eastern Africa. However, future FLDAS global and  
367 Central Asia versions can be run with Noah-Multi parameterization (Noah-MP) (Niu et al., 2011)  
368 which has multiple vegetation options and relies on either Leaf Area Index rather or GVF. This  
369 model update is expected to open possibilities for choice of datasets to meet our application needs  
370 and potentially improve representation of the water balance.

371 One important feature, added by the NASA LISF software development team, is the radiation  
372 correction described in Kumar et al. (2013), which improves the representation of snow dynamics  
373 with respect to slope and aspect corrections on the downward solar radiation field. The precipitation  
374 and other meteorological forcing variables, the period of record, and the spatial resolution were all  
375 determined to best meet the target end-users’ needs (i.e. FEWS NET) for routine agricultural and  
376 hydrologic monitoring.

377 Another noteworthy feature is the method of the Central Asia data stream restart (i.e., annual  
378 initialization based on climatology), which was developed to address an issue of excessive inter-  
379 annual snow accumulation found in the Noah LSM. First, a nine-year spin-up of the system was  
380 performed to produce stable snow and soil moisture conditions. Next, the resulting model states  
381 were compared with the Moderate Resolution Imaging Spectroradiometer (MODIS) Maximum  
382 Snow-Extent data originally computed by NOAA National Operational Hydrologic Remote Sensing  
383 Center (Personal Communication Greg Fall, 2014). Then, the model-estimated conditions were  
384 adjusted to produce a climatological model state for 1-October that is used to initialize each year.  
385 This approach ensures that the “water year”, beginning 1-October, is initialized with a reasonable  
386 amount of snowpack. While this method does effectively manage excessive inter-annual snow  
387 accumulation, the user should be aware that using the climatological model state will persist for 1-  
388 2 months in the water and energy balance of the LSM until they are superseded by “observed”  
389 meteorological inputs for the current water year. Preliminary work indicates that this issue will be  
390 resolved in future updates. In contrast, the global data stream does not employ this 1-October  
391 initialization procedure.

## 393 2.2 Meteorological Forcing Inputs

394 Precipitation is the most important input to the FLDAS products. The lower-latency Central Asia  
395 data stream is a daily product, forced with NOAA's Global Data Assimilation System (GDAS)  
396 (Derber et al., 1991) 3-hourly precipitation, which is available from 2001-present at <1-day latency.  
397 Meanwhile, the global data stream is driven by the daily CHIRPS precipitation product, which is  
398 available from 1981-present at ~5-day latency for CHIRPS Preliminary and ~1.5-month latency for  
399 CHIRPS Final. As mentioned earlier, lack of rainfall stations for bias correction of satellite-derived  
400 estimates and evaluation poses a major challenge. However, we find that the GDAS rainfall product  
401 and the CHIRPS rainfall product are adequate for routine monitoring and, along with additional  
402 sources of remote sensed information, important for convergence of evidence when making a best  
403 guess at land surface states and fluxes.

404  
405 As previously discussed, precipitation is a critical input to land surface models. The lower-latency  
406 Central Asia data stream is a daily product, forced with GDAS (Derber et al., 1991) 3-hourly  
407 precipitation, which is available from 2001 to present at <1-day latency. This dataset was chosen  
408 because of its latency. The global data stream is driven by the daily CHIRPS product (Funk et al.,  
409 2015), which is available from 1981 to present at ~5-day latency for CHIRPS Preliminary and ~1.5-  
410 month latency for CHIRPS Final. The CHIRPS products were chosen as inputs because of their  
411 proven performance in the literature, which has made it the "gold standard" for food and water  
412 security monitoring by organizations like FEWS NET, the World Food Program, and others who  
413 need up-to-date estimates and a 40+ year historical record. As mentioned earlier, lack of rainfall  
414 stations for bias correction of satellite-derived estimates and evaluation poses a major challenge.  
415 However, we find that the GDAS rainfall product and the CHIRPS rainfall product are adequate for  
416 routine monitoring and, along with additional sources of remote sensed information, are important  
417 for convergence of evidence when making a best estimate at land surface states and fluxes.

418  
419 Before the daily CHIRPS rainfall data can be used as input to the FLDAS models, the daily  
420 precipitation ~~must be~~ is pre-processed to a sub-daily timestep, using the LDT component of the  
421 LISLISF software. LDT temporally disaggregates the daily CHIRPS rainfall, using an approach  
422 similar to the North American LDAS precipitation temporal downscaling method (Cosgrove et al.,  
423 2003). For this approach, we use a finer timescale MERRA-2 precipitation timescale as a reference  
424 dataset to ~~represents~~ represent an accurate diurnal cycle. ~~Coarser~~ We note that this step in our  
425 methodology facilitates the solving of FLDAS water and energy balances at a sub-daily timestep.  
426 However, for Central Asia we do not have sufficient reference data available to assess the  
427 importance of sub-daily precipitation distribution, as was demonstrated by Sarmiento et al. (2021)  
428 for the United States where adequate reference data are available. For spatial downscaling, coarser  
429 scale meteorological forcings are spatially disaggregated to the output resolution (0.01, and 0.1  
430 degree for Central Asia and global, respectively) in the LISLISF using bilinear interpolation.

431  
432 The FLDAS models require additional meteorological inputs, including air temperature, humidity,  
433 radiation, and wind. The lower-latency Central Asia data stream uses GDAS 3-hourly

434 meteorological inputs available from 2001-present at <1-day latency. For a longer historical record,  
435 the global data stream of FLDAS uses NASA's Modern Era Reanalysis for Research and  
436 Applications version 2 (MERRA-2) (Gelaro et al., 2017) (1979-present) 1-hourly products with a  
437 two-week latency.

438 The FLDAS models require additional meteorological inputs, including air temperature, humidity,  
439 radiation, and wind. The lower-latency Central Asia data stream uses GDAS 3-hourly  
440 meteorological inputs available from 2001-present at <1-day latency. For a longer historical record,  
441 the global data stream uses MERRA-2 (Gelaro et al., 2017) (1979-present) 1-hourly products with a  
442 two-week latency. Over the Afghanistan domain GDAS temperature has an upward trend, whereas  
443 MERRA-2 is consistently warmer before 2010. We find that GDAS and MERRA-2 temperature  
444 estimates are of similar magnitude during 2011-2020. Similar results were noted by Yoon et al.  
445 (2019) who found an upward trend in GDAS temperature, as well as consistently higher  
446 temperatures in MERRA-2 across a broad High Asia domain.

### 447 2.3 Model Evaluation Statistics and Comparison Data

448 ~~To assess~~In addition to guidance from previous studies (Section 1.2), we assessed the quality of our  
449 modeling outputs, ~~we conduct by conducting~~ comparisons between (1) FLDAS satellite rainfall  
450 inputs and other satellite precipitation estimates, and (2) model estimated snow cover fraction and  
451 satellite derived snow cover fraction estimates.

452  
453 For the precipitation analysis, we compare CHIRPS and GDAS inputs to the Integrated Multi-  
454 satellite Retrievals for the Global Precipitation Mission (IMERG), a NASA precipitation product  
455 that integrates passive microwave and infrared satellite data with surface station observations  
456 (Huffman et al., 2020)(Huffman et al., 2020). The IMERG Final Run precipitation product,  
457 available at ~ 2-month latency (thus not suitable for our monitoring applications) has been used in  
458 numerous verification studies, including studies over Africa (Dezfuli et al., 2017)(Dezfuli et al.,  
459 2017), South America (Gadelha et al., 2019; Manz et al., 2017)(Gadelha et al., 2019; Manz et al.,  
460 2017), and the mid-Atlantic region of the United States (Tan et al., 2016). These studies  
461 demonstrated that IMERG Final (Tan et al., 2016). These studies demonstrated that IMERG Final  
462 Run was able to capture large spatial patterns and seasonal and interannual patterns of rainfall.  
463 However, fewer studies have explored the performance of the lower latency IMERG Late Runs  
464 (DOI Run (doi: 10.5067/GPM/IMERGDL/DAY/06) product that we use here. Kirshbaum et al.  
465 (2016) include a qualitative comparison for CHIRPS Final and IMERG Late Run for the Southern  
466 Africa start-of-season 2015. IMERG Late Run appears to perform similarly to the 1.5-month latency  
467 CHIRPS Final and outperform the 1-day latency NOAA Rainfall Estimate version 2 (RFE2) product  
468 (Xie and Arkin, 1996)(Xie and Arkin, 1996). Differences in the daily rainfall distribution patterns  
469 between IMERG Final Run and CHIRPS Final have also been shown to ~~impact~~affect the resulting  
470 hydrological modeled output in simulations done using the NASA LIS framework LISF (Sarmiento  
471 et al., 2021).

473 For the ~~Snow-Cover-Fractions~~ snow cover fraction (SCF) analysis, we compare the global and Central  
474 Asia data streams with the MODIS daily SCF product, MOD10A1 Collection 6 (~~Hall and Riggs,~~  
475 ~~2016~~) (Hall and Riggs, 2016). MOD10A1 data ~~is~~ are available at 500-m spatial resolution from  
476 February 2000 to the present. SCF is generated using the Normalized Difference Snow Index  
477 (NDSI) and additional filters to reduce error and flag uncertainty. Routine qualitative comparisons,  
478 which can be viewed on the NASA ~~LISLISF~~ FEWS NET project website, generally show  
479 agreement between the model and MODIS SCF, as well as occurrence of cloud cover  
480 (<https://ldas.gsfc.nasa.gov/ldas/models/central-asia>). Following Arsenault et al. (2014), we  
481 aggregated pixels to 0.01 degree to reduce error related to sensor viewing angles and gridding  
482 artifacts. For this analysis, using MODIS SCF as “truth”, we determined True Positives (TP), True  
483 Negatives (TN), False Negatives (FN) and False Positives (FP). We then computed probability of  
484 detection (POD) where  $POD = (TP / (TP + FN))$  and False Alarm Rate (FAR) where  $FAR =$   
485  $(FP / (FP + TN))$ . We computed these for the total area of Afghanistan, (60-76E, 28-39N), as well as  
486 by basin (Fig. 3-a & b-4). This paper does not compare modeled snow water equivalent (SWE) to  
487 independent snow observations because, as noted by Yoon et al. (2019), direct evaluation of snow  
488 mass and ~~snow-water-equivalent~~ (SWE) is difficult over Central Asia due to poor coverage of  
489 accurate snow observations. We follow the Yoon et al. (2019) recommendation to conduct  
490 quantitative SCF comparisons and provide qualitative SWE analysis in Applications, Section 4.

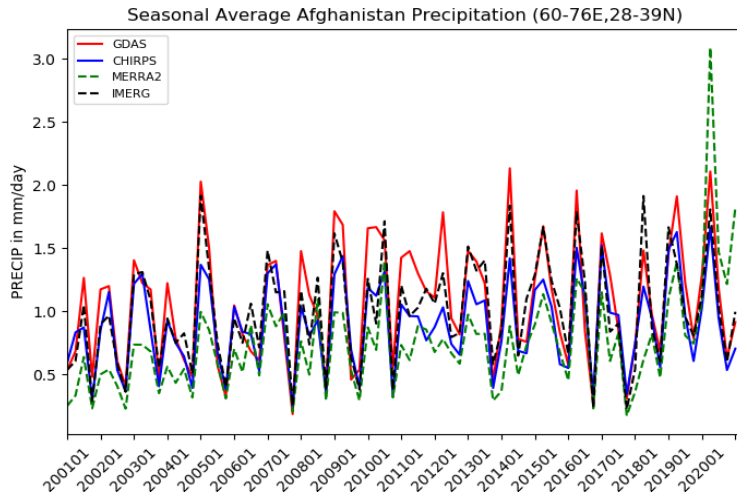
491  
492 In addition to rainfall and snow comparisons, we conducted monthly pixel-wise comparison of  
493 Central Asia and the global run’s estimates of evapotranspiration (ET) and soil moisture versus  
494 Operational Simplified Surface Energy Balance (SSEBop, (Senay et al., 2013)), ET and Soil  
495 Moisture Active Passive (SMAP) Level 3 (Entekhabi et al., 2010, 2016) using the Normalized  
496 Information Contribution (NIC) metric following Sarmiento et al., (2021). The analysis was  
497 performed for the period 2016-2021 to match the SMAP record. The NIC metric first computes  
498 anomaly correlations between the model runs and the reference dataset and then computes the  
499 difference between the performance of each model run using a scale of -1 to +1 to highlight if the  
500 global or Central Asia data stream performs better with respect to the reference. To make the  
501 comparisons, the reference datasets (SMAP and SSEBop) were re-gridded to match the grid spacing  
502 and locations of the experiment model outputs.

### 503 3 Results

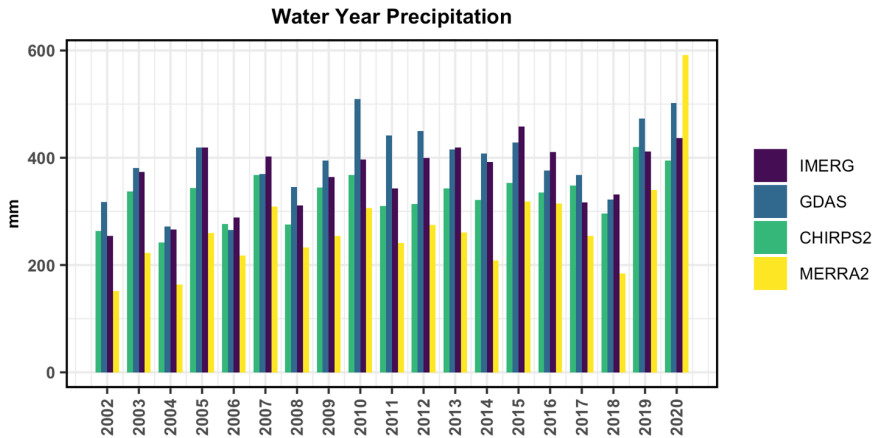
#### 504 3.1 Gridded Rainfall Comparison

505 ~~For~~ We have two data streams for Central Asia applications ~~we have two data streams~~ with different  
506 precipitation inputs: 1) the global data stream with CHIRPS precipitation at 10-km<sup>2</sup>-km spatial  
507 resolution provides a long-term consistent data record; and 2) the Central Asia data stream with  
508 GDAS precipitation at 1-km<sup>2</sup>-km provides near real time, finer spatial resolution updates. These two  
509 data streams have their respective errors and allow data users to apply a convergence of evidence  
510 approach for food and water security applications. ~~In this~~ This section ~~we present~~ presents a  
511 comparison of ~~these~~ the GDAS, and CHIRPS precipitation inputs used for the Central Asia and

512 global data streams, respectively. We also include IMERG Late Run for comparison as a high  
 513 quality, low latency product. Future work will may incorporate the IMERG Late Run precipitation  
 514 inputs into FLDAS simulations. We also include MERRA-2 precipitation for comparison. Pair-wise  
 515 correlation correlations are shown in Table 2. CHIRPS Final, IMERG Late Run and GDAS ( $R \geq$   
 516 0.90) are well correlated in terms of average daily precipitation (mm/day) at the monthly and annual  
 517 (i.e., water year) timestep. MERRA-2 correlations with these datasets are lower at the monthly  
 518 timestep ( $0.75 \leq R \leq 0.81$ ) and annual timestep water year ( $0.64 \leq R \leq 0.69$ ) timesteps. Fig. 4  
 519 shows the time series of the precipitation products for their overlapping period of record (2001-  
 520 2020), which illustrates how they co-vary in time, and shows some general patterns in terms of  
 521 relative precipitation in mm/day: GDAS (red/blue) and IMERG Late (dashed-black/Run (purple)) tend  
 522 to have the highest average precipitation per day totals, CHIRPS (blue/green) has lower  
 523 mm/day precipitation but is higher than MERRA-2 (dashed-green/yellow) which tends to have the  
 524 lowest average precipitation per day, until 2019 when it is notably higher than the other products.



525  
 526



527  
528  
529  
530  
531  
532  
533  
534

Figure 4. Afghanistan country-wide average, annual average mm/day time-series water year precipitation for CHIRPS, GDAS, IMERG Late Run, and MERRA-2. At the annual time step, Spearman rank correlations range from 0.64 (GDAS vs. MERRA-2) to 0.92 (GDAS vs. CHIRPS).

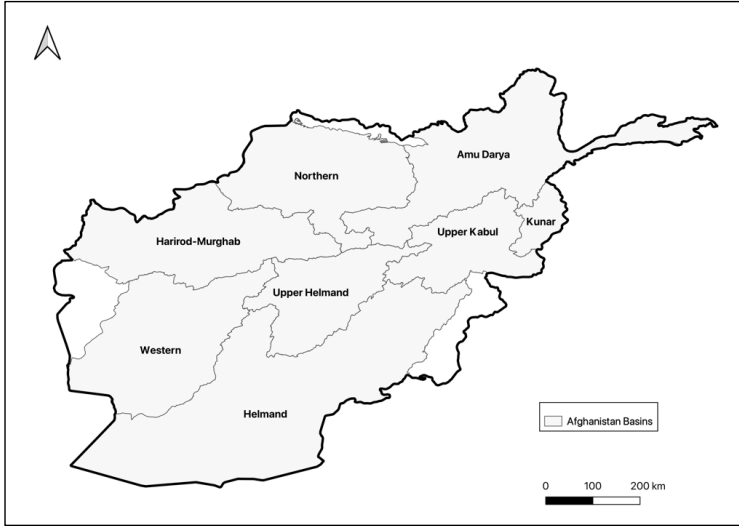
Table 2. Afghanistan spatial average Spearman Rank Correlation (R) of monthly (annual water year) precipitation 2001-2020

	GDAS	CHIRPS Final	IMERG Late Run
GDAS	x	-	-
CHIRPS Final	0.91 (0.92)	x	-
IMERG Late Run	0.91 (0.89)	0.92 (0.90)	x
MERRA-2	0.75 (0.64)	0.78 (0.68)	0.81(0.69)

535

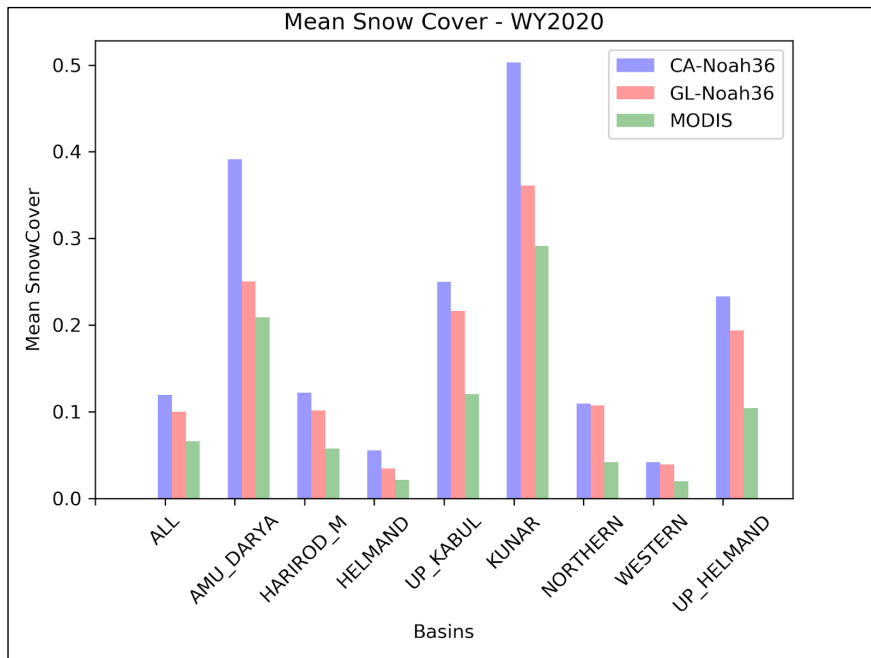
### 536 3.2 Remotely Sensed and Modeled Snow comparisons

537 The estimation of snow is important for Afghanistan and Central Asia because it is an important  
538 critical contributor to water resources and irrigated agriculture. Here, we compare mean We  
539 compared average SCF (Fig. 5a6a), POD, and FAR statistics (Fig. 5b6b) relative to MODIS SCF  
540 over eight hydrologic basins in Afghanistan.  
541



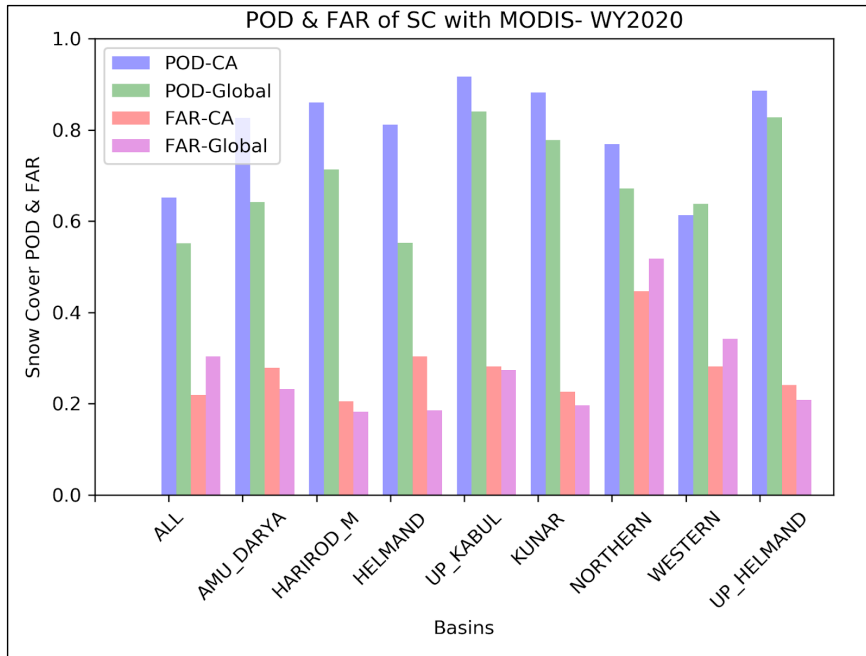
542  
543  
544  
545

Figure 5. Hydrologic basins used in the analysis of categorical statistics for snow covered fraction.



546 Figure 5a6a. Mean snow cover fraction for the entire area and by hydrologic basin for MODIS  
 547 Snow Cover Fraction (SCF), Central Asia (CA) and global (GL) data streams for water year 2020.  
 548



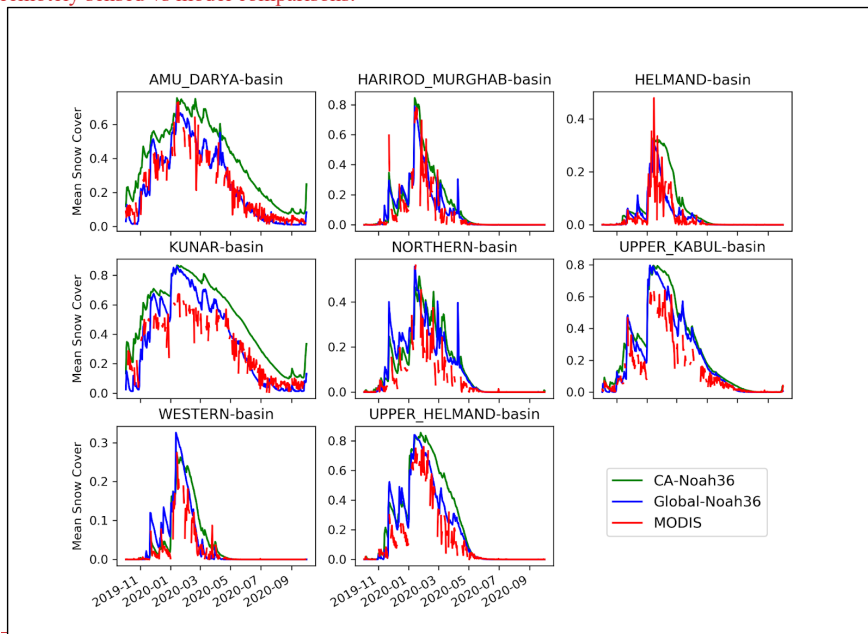


549 Figure 5b6b. Probability of Detection (POD) of snow presence, and False Alarm Rate (FAR) for the  
 550 Central Asia (CA) and global data streams relative to the MODIS SCF for water year 2020.  
 551  
 552

Formatted: Font color: Auto

553 Overall, both model runs estimate greater meanaverage SCF than the MODIS SCF product. The  
 554 Central Asia (CA) data stream has consistently higher meanaverage snow cover for all basins  
 555 compared to MODIS SCF estimates and the global data stream. Perhaps not surprisingly then it that  
 556 the Central Asia data stream performs consistently better in POD (by basin = ~80%) except for the  
 557 Western [Helmand] Basin. Similarly, the FAR of the CA Central Asia data stream is higher where  
 558 POD is higher except for the Northern Basin. The difference in statistics may be related to the  
 559 different inputs forcing inputs or the higher spatial resolution of the Central Asia data stream.  
 560 Kumar et al. (2013) note that higher spatial resolution was important for snow dominated basins.  
 561 We also note the likely importance of the MERRA-2 and GDAS temperature forcing between the  
 562 global data stream and the Central Asia data stream, respectively. The panels in Fig. 6 provide  
 563 additional insight into the differences between MODIS SCF and the two FLDAS runs for water year  
 564 2020. The green line (Central Asia) is consistently higher than the red, MODIS SCF estimates, and  
 565 the blue, global data stream estimates. Both the models estimate higher SCF during peak coverage

566 in the Upper Kabul and Kunar basins. The time series plots also illustrate discontinuities in the  
567 MODIS SCF time series, likely related to cloud-cover, which reduced the sample size for the  
568 remotely sensed vs model comparisons.



569 Figure 6. Basin-averaged SCF for Water Year 2020 as estimated by global and Central Asia (CA)  
570 data streams, and MODIS SCF. Time series show generally a similar pattern with the CA typically  
571 having higher SCF values. These plots also demonstrate discontinuities in the MODIS SCF data that  
572 reduce the quality of quantitative comparisons but provide qualitative confirmation of adequate  
573 model performance.  
574

### 575 3.3 Discussion of results compared to previous studies

576 Despite the lack of ground-based observations, our analysis shows that the remotely sensed  
577 estimates and the models have good correspondence with other sources of evidence in terms of  
578 seasonal timing and performance. This provides analysts with confidence when using the FLDAS  
579 snow estimates, in tandem with other sources, as an input to food security analysis. Our approach is  
580 supported by other studies that have explored the challenges of evaluating hydrologic estimates over  
581 the region (Yoon et al., 2019; Ghatak et al., 2018; Immerzeel et al., 2015; Qamer et al., 2019). With  
582 a study domain shifted to the east, Yoon et al. (2019) evaluate rainfall and near surface temperature

583 estimates over the High Mountain Asia domain, including most of Afghanistan. They review how  
584 these results compare to other studies (e.g. precipitation trends (Nguyen et al., 2018; Rodell et al.,  
585 2018)), and their results suggest that the uncertainty in the meteorologic forcing is the dominant  
586 factor in the terrestrial water budget estimates. This is consistent with our results showing  
587 differences between the GDAS and CHIRPS+MERRA-2 driven outputs. Also consistent with our  
588 results, Yoon et al. (2019) show that their LSM ensembles of SCF have an average POD of 72% and  
589 FAR of 36%, which is within the range of our POD and FAR statistics (60-80% POD; 20-40%  
590 FAR) compared to MODIS SCF. Without a clear “winner” in their multi-model and multi-forcing  
591 experiments, Yoon et al.  
592 In addition to precipitation and snow cover comparisons we conducted comparisons with remotely  
593 sensed soil moisture and ET (not shown). We found that in general, GDAS derived estimates of ET  
594 consistently performed better over Afghanistan in terms of pixel-wise anomaly correlation and NIC  
595 with SSEBop ET. Meanwhile, neither modeled estimate of soil moisture consistently outperformed  
596 the other with respect to SMAP. The ET results lend some support to the quality of the Central Asia  
597 data stream estimates. However, the lack of signal in the soil moisture comparisons suggests that  
598 more careful analysis of the model and remote sensing errors is required before drawing conclusions  
599 regarding which data stream is “best.”

### 600 **3.3 Discussion of results compared to previous studies**

601 Despite the lack of ground-based observations, our analysis shows that the remotely sensed  
602 estimates and the models have good correspondence with other sources of evidence in terms of  
603 seasonal timing and performance. This provides analysts with confidence when using the FLDS  
604 snow estimates, in tandem with other sources, as an input to food security assessments. Our  
605 approach is supported by other studies that have explored the challenges of evaluating hydrologic  
606 estimates over the region (Immerzeel et al., 2015; Ghatak et al., 2018; Yoon et al., 2019; Qamer et  
607 al., 2019).

608  
609 Yoon et al. (2019) show that their LSM ensembles of SCF have an average POD of 72% and FAR  
610 of 36%, which is within the range of our POD and FAR statistics (60-80% POD; 20-40% FAR)  
611 compared to MODIS SCF. The categorical statistics indicate that Central Asia (GDAS) tends to  
612 have both a higher probability of detection and false alarm rate, indicating higher averages than  
613 MODIS SCF and global (CHIRPS).

614  
615 With respect to the soil moisture and ET comparisons, we found that the Central Asia data stream  
616 estimates of ET were better correlated with SSEBop ET, but neither data stream was consistently  
617 better correlated with SMAP. These differences could be a function of non-precipitation differences,  
618 or higher spatial resolution. Ghatak et al. (2018) also found that the choice of reference dataset (with  
619 its own characteristics and errors) was an important factor.

620

In general, given the lack of clarity on “best” FLDAS data stream, the convergence of evidence approach allows us to consult both data streams, leveraging the longer time series of CHIRPS and the lower latency of GDAS.

### 3.4 Limitations and Future Developments

~~conclude that improvements in the meteorological boundary conditions would be needed to reduce the uncertainty in the terrestrial budget estimates. These sentiments are echoed in Qamer et al. (2019).~~

One recent attempt to improve meteorological inputs in the region is from Ma et al. (2020) with the development of the AIMERG dataset that combines IMERG Final with APHRODITE (Asian Precipitation—Highly-Resolved Observational Data Integration Toward Evaluation) rain-gauge derived product (Yatagai et al., 2012). Ultimately, it would be beneficial to have a global modeling system that used the best available inputs from each region. In the meantime, multi forcing and multi-model ensembles, and convergence of evidence with other remotely sensed data and field reports, are a viable approach for providing hydrologic estimates for various applications.

### 3.4 Summary of differences between the model runs

Given the need for multiple data streams for convergence of evidence, we have summarized the pros and cons of the Central Asia and global data streams in Table 3.

Table 3. Pros and cons of the two data streams

	Central Asia: Noah 3.6 with GDAS (2000-present)	Global: Noah 3.6 with CHIRPS+MERRA-2 (1982-present)
PROS Pros	1 km <sup>2</sup> -km	less computationally intensive
	1-day latency, daily timestep	longer time record
	Snow estimates available in USGS Early Warning eXplorer <a href="https://earlywarning.usgs.gov/fews/ewx/">https://earlywarning.usgs.gov/fews/ewx/</a>	CHIRPS & MERRA-2 forcing spatial resolution does not change over time (stable climatology)
		Water and Energy balance available in NASA GIOVANNI; <a href="https://giovanni.gsfc.nasa.gov/giovanni/">https://giovanni.gsfc.nasa.gov/giovanni/</a> ; Google Earth Engine; <a href="https://developers.google.com/earth-engine/datasets/tags/fldas">https://developers.google.com/earth-engine/datasets/tags/fldas</a> ; Climate Engine <a href="https://climateengine.com/">https://climateengine.com/</a>

Formatted: Font: +Body (Times New Roman)

Formatted: Font: +Body (Times New Roman)

Formatted: Font: +Body (Times New Roman)

Formatted: Font: +Body (Times New Roman)

Formatted Table

CONSCons	more computationally intensive	lower resolution (10 <del>km</del> <sup>2</sup> -km)
	shorter time record	~30-day latency
	GDAS forcing resolution changes over time (unstable climatology) (NOAA NCEP <a href="https://www.emc.ncep.noaa.gov/gmb/STATS/html/model_changes.html">https://www.emc.ncep.noaa.gov/gmb/STATS/html/model_changes.html</a> )	not publicly available at daily timestep
	large data volume, difficult to move	

Formatted: Font color: Auto

Formatted: Font color: Auto

Formatted: Font color: Auto

641

642

643

644

645

646

647

648

649

650

651

652

653

654

655

656

657

658

659

660

661

662

663

664

665

666

667

IMERG version 6 was released in 2019 and includes rainfall estimates processed back to 2000. Prior to this change we had found encouraging results when comparing the onset of rainy season using both IMERG Late Run and CHIRPS (Kirschbaum et al., 2016). However, at that time the period of record was a limitation for computing anomalies. We now have an adequate period of record, and IMERG Late Run is planned to be part of the upcoming FLDAS global and FLDAS Central Asia releases. We are also encouraged by the quality of IMERG at the daily timestep when compared to CHIRPS over the United States where accurate reference data are available (Sarmiento et al., 2021).

In addition to IMERG other promising rainfall datasets are in development. Ma et al. (2020) have developed the AIMERG dataset that combines IMERG Final Run with the APHRODITE rain-gauge derived product (Yatagai et al., 2012). Another promising dataset is CHIMES (Funk et al., 2022), a blend of CHIRPS and IMERG, whose developers have been exploring the strengths and limitations of these two datasets and their fusion to produce an optimal product.

With respect to other FLDAS developments, FLDAS global and Central Asia are planned to be transition to Noah-MP. This will allow for improved representation of snowpack and groundwater. This will also necessitate the use of different parameters, e.g., leaf area index, as well as the potential to explore different parameter sets like ISRIC soils. In the meantime, multi-forcing and multi-model ensembles, and convergence of evidence with other remotely sensed data and field reports, are a viable approach for providing hydrologic estimates for various applications.

Formatted: Font: +Body (Times New Roman)

Formatted: Font: +Body (Times New Roman)

Formatted: Font: +Body (Times New Roman)

Formatted: Font color: Auto

#### 4 Applications

These data from global and Central Asia data streams are routinely used in several FEWS NET information products listed in Table 4. ~~There is a weekly briefing from~~ NOAA's Climate Prediction Center (CPC) International Desks provide a weekly briefing on the past week's weather conditions and 1–2-week forecasts for FEWS NET regions of interest, including Central Asia. There is also a monthly FEWS NET Seasonal Monitor and a monthly Seasonal Forecast Review for which

668 these data provide information on the current state of the snowpack, soil moisture, and runoff. These  
 669 "observed conditions" can then be qualitatively combined with forecasts ranging from 1 week to  
 670 3many months in the future to assess potential hydro-meteorological hazards. To demonstrate the  
 671 role of these data in the early warning process, at different points in the season, we provide an  
 672 example of the 2017-2018 wet season in Afghanistan during a La Niña event that contributed to  
 673 drought.

Formatted: Font color: Auto

674  
 675 Table 4. Routine Applications of FLDAS Central Asia’s Afghanistan hydrologic data.

Routine application of these data	Weblink to updates	Notes
FEWS NET Global Weather Hazards Summary produced by NOAA CPC	<a href="https://fews.net/global/global-weather-hazards/">https://fews.net/global/global-weather-hazards/</a> <a href="https://www.cpc.ncep.noaa.gov/products/international/index.shtml">https://www.cpc.ncep.noaa.gov/products/international/index.shtml</a>	shapefiles <a href="https://ftp.cpc.ncep.noaa.gov/fews/weather_hazards/">https://ftp.cpc.ncep.noaa.gov/fews/weather_hazards/</a>
USGS-Seasonal Monitor	<a href="https://earlywarning.usgs.gov/fews/search/Asia/Central%20Asia/Afghanistan">https://earlywarning.usgs.gov/fews/search/Asia/Central%20Asia/Afghanistan</a>  Archives: <a href="https://fews.net/sectors-topics/sectors/agroclimatologyhttps://earlywarning.usgs.gov/fews/afghanistan/seasonal-monitor">https://fews.net/sectors-topics/sectors/agroclimatologyhttps://earlywarning.usgs.gov/fews/afghanistan/seasonal-monitor</a>	Updated monthly near the middle of each month from October - May, during the precipitation wet season.
FEWS NET Food Security Outlook Brief	<a href="https://fews.net/central-asia/afghanistan">https://fews.net/central-asia/afghanistan</a>	Information on snow or other hydrology included if applicable
Crop Monitor for Early Warning	<a href="https://cropmonitor.org/index.php/cmreports/early-warning-report/">https://cropmonitor.org/index.php/cmreports/early-warning-report/</a>	Information on early warning and crop conditions

Formatted Table

Formatted: Font color: Auto

Formatted: Font color: Auto

Formatted: Font color: Auto

676

677 **4.1 Snow monitoringMonitoring & Seasonal Outlooks**

678 As previously mentioned, and as shown in Fig. 7, Afghanistan and the broader region is strongly  
 679 influenced by La Niña, which tends to increase the likelihood of dry events (Barlow et al., 2016;  
 680 FEWS NET, 2020b). Depending on other factors, this may also increase the probability of negative  
 681 snowpack anomalies, reduce springtime streamflow, and flood risk, and reduce summer irrigation  
 682 availability and potentially crop yields<sup>7</sup>. Afghanistan and the broader region is strongly influenced  
 683 by La Niña, which tends to increase the likelihood of below average precipitation. Depending on  
 684 this and antecedent conditions there in an increased likelihood of below average snowpack, reduce  
 685 springtime streamflow and flood risk, reduce summer irrigation water availability, and crop yield  
 686 losses.

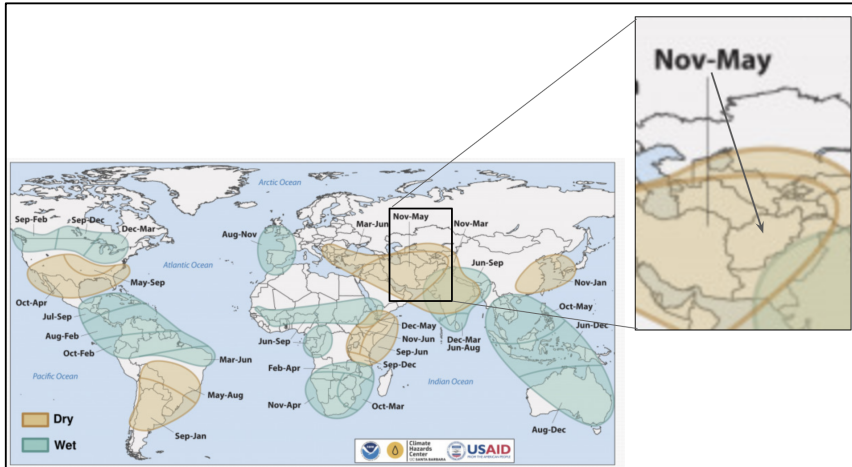


Figure 7. Timing of wet and dry conditions related to La Niña. Increased likelihood of dry conditions from ~~Nov~~~~November~~-May for Afghanistan during La Niña events.

Formatted: Font color: Auto

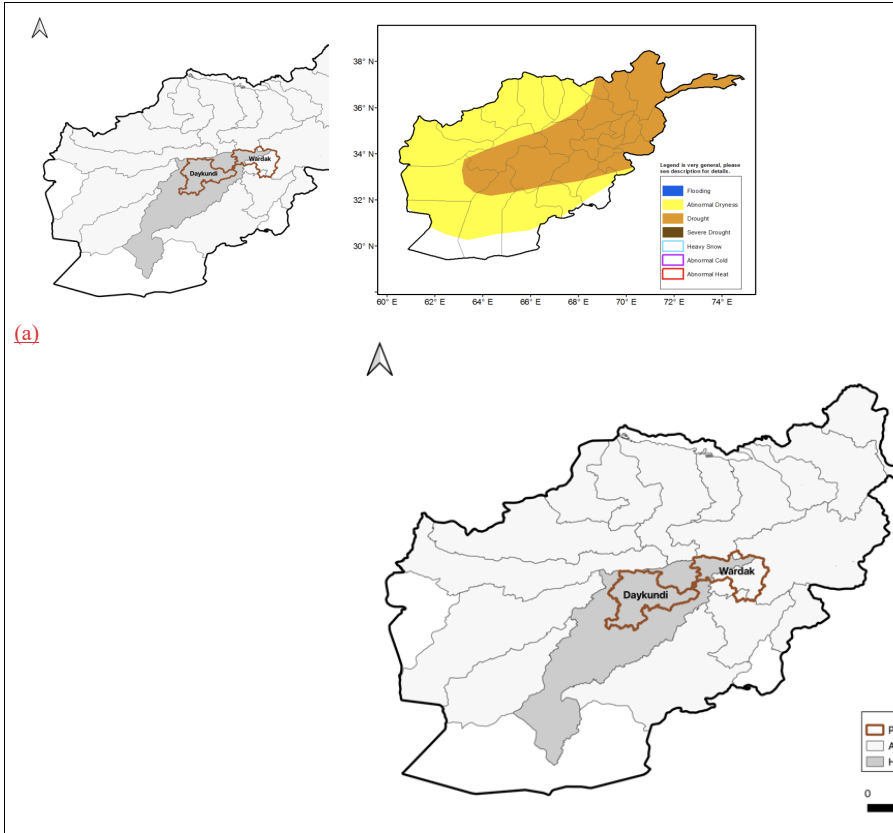
A La Niña Watch was issued by NOAA in September 2017 (NOAA, 2017). The FEWS NET October 2017 Food Security Outlook (FEWS NET, 2017a) stated that La Niña conditions were expected throughout the northern hemisphere fall and winter and that below-average precipitation was likely over much of Central Asia, including Afghanistan, during the 2017-2018 wet season. With the expectation of below average ~~rainfall~~~~precipitation~~ coupled with above average ~~temperature forecasts~~~~temperatures~~, FEWS NET anticipated that snowpack would most likely be below average. In the context of food security outcomes, it was assumed that areas planted with winter wheat were likely to be ~~lower~~~~less~~ than usual, reducing land preparation activities and associated demand for labor. Two provinces of particular concern were Daykundi and Wardak (Fig. 8a brown borders), both located in the Helmand River Basin (Fig. 8a; ~~grey~~~~gray~~ shading). Precipitation deficits in these provinces would lead to poor rangeland resources and pasture availability and would likely result in decreased livestock productivity and milk production through May. However, given that October was the ~~very~~ start of the wet season, there remained a large spread of possible outcomes: spatial and temporal rainfall distributions, and snowpack totals necessitating routine updates to assumptions.

Formatted: Font color: Auto

Monitoring continued ~~onward~~~~in~~~~during~~ the ~~wet~~ season ~~from~~~~October~~, tracking observations from remote sensing, models, and field reports as well as ~~weather, sub-seasonal and seasonal~~ forecasts ~~across timescales~~. This information was used to regularly update expectations of end of season outcomes. Using the FLDAS Central Asia data stream, a December 21, 2017, NOAA CPC Weather Hazards Brief reported that parts of northern and central Afghanistan remained atypically snow free, and north-eastern high elevation areas exhibited ~~snow~~~~water~~~~equivalent~~ (~~SWE~~) deficits. SWE is a

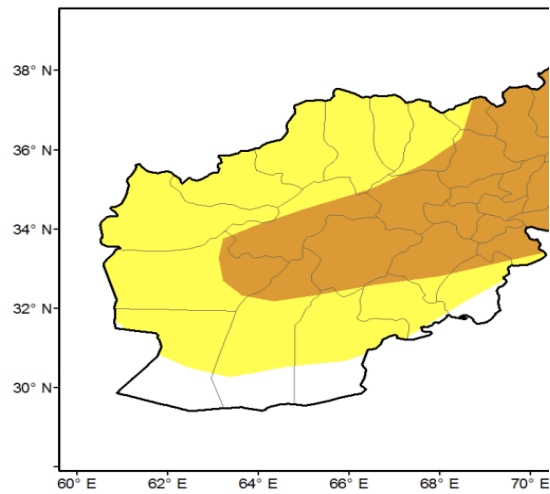
712 commonly used measurement of the amount of liquid water contained within the snowpack, and an  
713 indicator of the amount of water that will be released from the snowpack when it melts. By January  
714 17, 2018, an abnormal dryness polygon was placed over ~~northeast~~northeastern Afghanistan; ~~and~~  
715 the central highlands ~~of Afghanistan~~, based on below-average ~~snow water equivalent~~SWE values from  
716 the FLDAS Central Asia estimates. Abnormal dryness is defined for an area that has registered  
717 cumulative 4-week precipitation and soil moisture ranking less than the 30th percentile, with a  
718 Standardized Precipitation Index (SPI) of 0.4 standard deviation below the mean~~average~~. In  
719 addition, it is required that forecasts indicate below-average precipitation (less than 80% of normal)  
720 for that area during the 1-week outlook period. By late February 2018, precipitation deficits and  
721 related SWE (Fig. 9) increased and met the criteria for “drought” (Fig. 8b). Drought is defined as an  
722 area that has previously been defined as “Abnormal Dryness” and has continued to register seasonal  
723 precipitation and soil moisture deficits since the beginning of the rainfall season. Specifically, an  
724 eight-week cumulative precipitation, soil moisture, and runoff below the 20th percentile rank, and  
725 an SPI of 0.8 standard deviation below the mean~~average~~ are classification guidelines.  
726





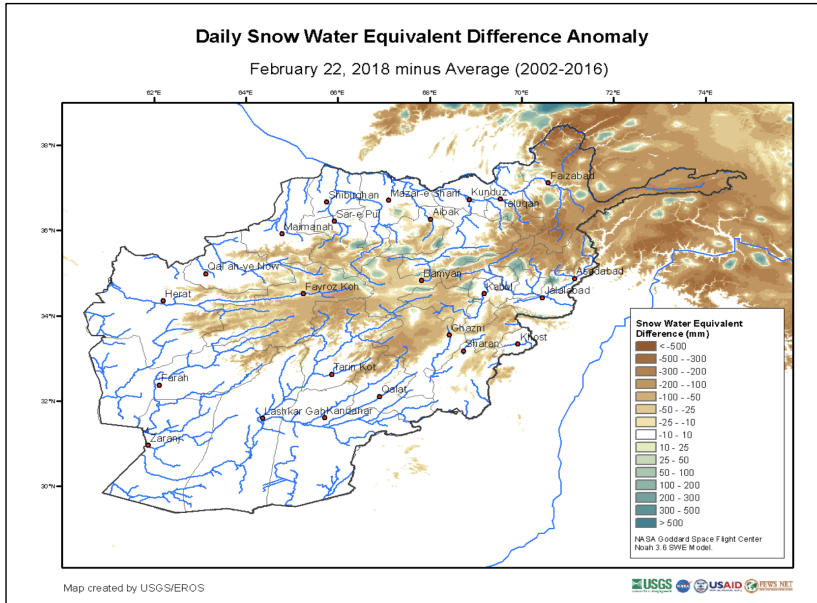
Formatted Table

(b)



727

728 Figure 8. (a) Map showing hydrological basins, with Helmand Basin in darker grey and  
729 location of Daykundi and Wardak provinces (outlined in red) where food security conditions were  
730 of particular concern. (b) NOAA CPC Afghanistan Hazard Hazards Report for February 22-28, 2018  
731 (CPC NOAA, 2018); map showing widespread abnormal dryness and drought, defined by 90-day  
732 precipitation deficits and extremely low snow water equivalent.  
733

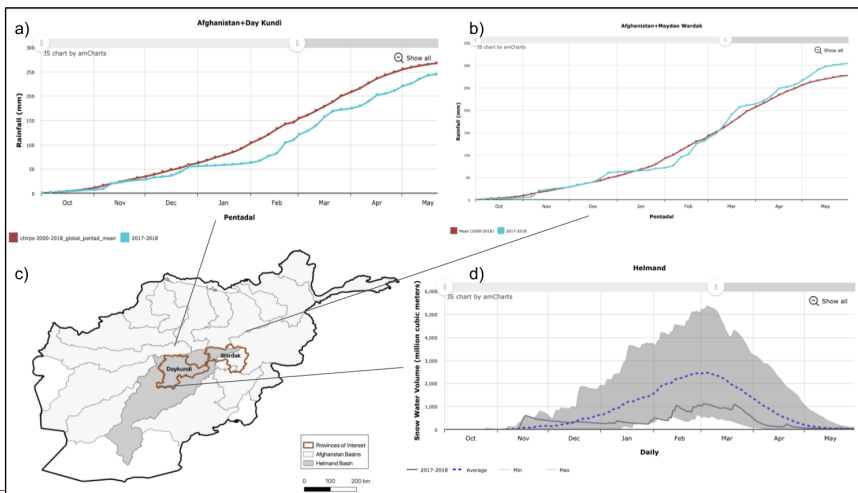


734  
735 Figure 9. FLDAS Central Asia snow water equivalent (SWE) estimates for February 22, 2018.  
736 SWE deficits of  $\geq 300$ -mm were widespread at this time.  
737

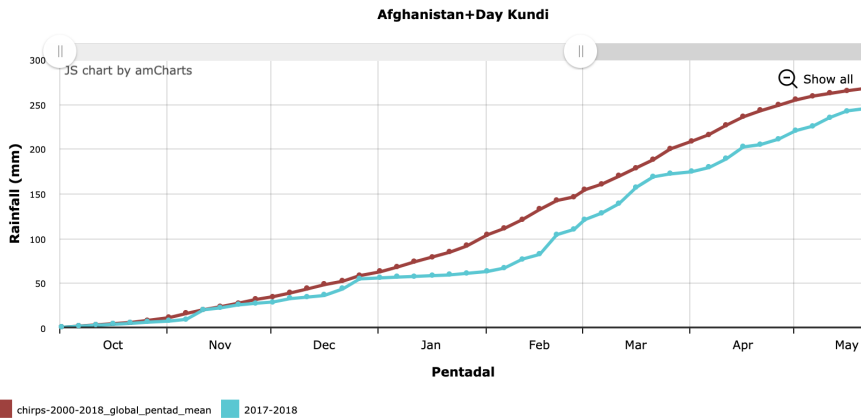
738 The February 2018 Food Security Outlook (FEWS NET, 2018b) provided the following updates,  
739 based on the CPC Hazards Reports and Seasonal Monitors: “Snow accumulation and cumulative  
740 precipitation were well below average for the season through February 2018, with some basins at or  
741 near record low snowpack, with data since 2002....These factors will likely have an adverse impact  
742 on staple production in marginal irrigated areas and in many rainfed areas. [Moreover, with]  
743 forecasts for above-average temperatures during the spring and summer, rangeland conditions are  
744 expected to be poor during the period of analysis through September 2018. This could have an  
745 adverse impact on pastoralists and agro-pastoralists, particularly in areas where livestock  
746 movements are limited by conflict.” The Crop Monitor for Early Warning reports for February and  
747 March 2018 reports (GEOGLAM, 2018a, b) also cited reduced snowpack in Afghanistan and the  
748 negative impacts on winter wheat crops as well as irrigation water availability in the Spring. The  
749 story was also highlighted in NASA Earth Observatory March 2018 “Record Low Snowpack in  
750 Afghanistan” (Record Low Snowpack in Afghanistan NASA Earth Observatory, 2018).  
751

Field Code Changed

752 The USGS's USGS Early Warning eXplorer (EWX) (Shukla et al., 2021)(Shukla et al., 2021) allows  
 753 analysts to look at maps and time series for a variety of variables and specific provinces and river  
 754 basins. Plots from EWX in Fig. 10 show below average precipitation ~~in~~for provinces in the Helmand  
 755 Basin for January and February. CHIRPS cumulative rainfall for 2017-18 ~~vs~~versus the 18-year  
 756 average for Day Kundi (a.k.a. Daykundi) Province showed near average conditions until December.  
 757 From January, cumulative rainfall remained below the 2000-2018 average throughout the rest of the  
 758 season ending in May; the same pattern occurred in nearby Uruzgan Province. In neighboring  
 759 Maydan Wardak (a.k.a Wardak) Province, below average conditions were experienced in January and  
 760 February, but cumulative rainfall recovered in March to remain slightly above average. Day  
 761 Kundi (Fig. 10a10b) and Wardak (Fig. 10b10c) are provinces located in the upper reaches of the  
 762 Helmand Basin. Fig. 10d10c shows SWE averaged across the entire Helmand basin. The greygray  
 763 shading indicates the range of the minimum and maximum values, and the dashed blue line is the  
 764 average. Initial snow conditions start above average until December ~~when, after which~~ SWE deficits  
 765 are near record low values through the beginning of February, and then persist at below-average  
 766 levels.  
 767

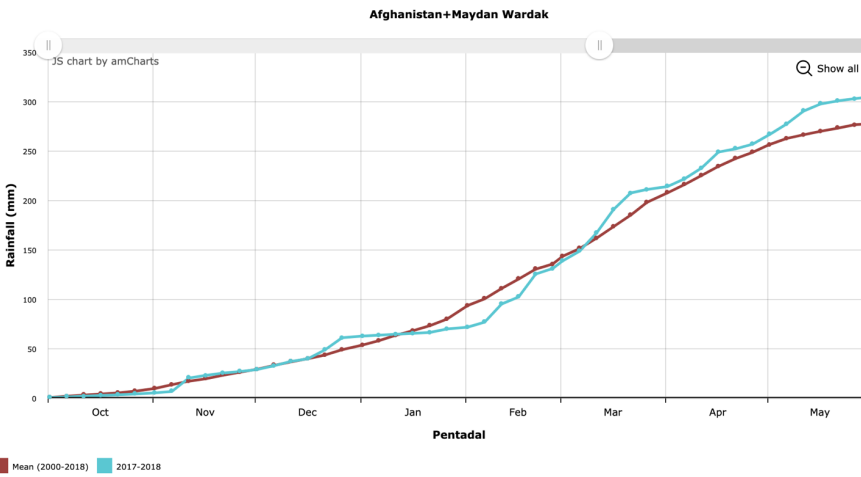


768



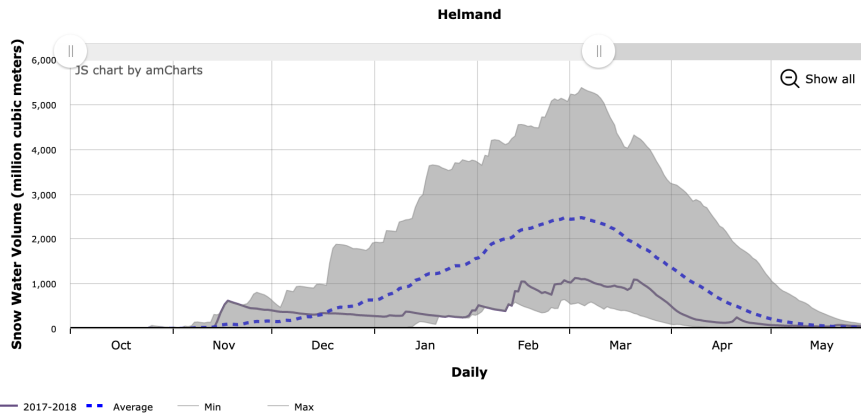
769  
770  
771  
772

Figure 10a. CHIRPS cumulative rainfall for 2017-18 versus average conditions for (a) Daykundi Province. (b). Figure from USGS EWX (<https://earlywarning.usgs.gov/fews/ewx/>).



773  
774  
775  
776

Figure 10b. CHIRPS cumulative rainfall for 2017-18 versus average conditions for Maydan Wardak Province. (c) Map showing location of Daykundi and Wardak provinces, and the Figure from USGS EWX (<https://earlywarning.usgs.gov/fews/ewx/>).



778

779

780

781

782

783

784

785

786

787

788

789

790

791

792

793

794

795

796

797

798

799

800

801

802

Figure 10c. Helmand Basin where food security conditions were of particular concern. (d) Helmand Basin snow water equivalent (SWE) from the Central Asia data stream. The grey shading indicates the range of the minimum and maximum values, dashed blue line is the average, and black line is 2017-18. Figure from USGS EWX (<https://earlywarning.usgs.gov/fews/ewx/>).

By the end of the season in April 2018, FEWS NET (2018c) concluded that “below-average precipitation throughout most of the country during the October 2017 – May 2018 wet season has led to very low snowpack ...Low irrigation water availability is likely to have an adverse impact on yields for winter wheat and other ...barley, maize, and others.. particularly in downstream areas in regions with limited rainfall. ...The poor performance of the wet season and above average temperatures... exacerbated dry rangeland conditions in many areas, particularly in ...Sari Pul, [and surrounding] ...provinces. Pastoralists and agropastoralists in these areas will likely attempt to migrate to areas with better pasture and water availability or sell livestock at below-average prices.” At the same time UNICEF reported in April 2018 (500,000 children affected by drought in Afghanistan—UNICEF, 2018) At the same time, UNICEF (2018) reported in April 2018 that among “the [drought] affected provinces, Baghis, Bamyan, Daykundi, Ghor, Helmand, ... and Uruzgan are of critical priority for nutrition and water, sanitation and hygiene assistance.”

Formatted: Font color: Auto

Several months after a season has ended, and harvest has ended is complete, more statistics become available for further verification of the drought outcomes. The FEWS NET October 2018 Food Security Outlook (2018a) reported that the 2017-18 drought had significant negative impacts on rainfed wheat production and livestock pasture and body conditions across the country. Reporting statistics from the Afghanistan Ministry of Agriculture, Irrigation, and Livestock, the total wheat production for the 2017-18 agriculture season was about 20% below average, where irrigated

803 agriculture performed about average. However, rainfed ~~agriculture~~~~agricultural~~ production was only  
804 about 50% of average, most severely ~~impacting~~~~affecting~~ households in ~~in~~ Badakhshan, Badhis, and  
805 Daykundi provinces ~~where. In these locations~~ dry conditions, ~~insecurity~~~~conflict~~, poor incomes, and  
806 depleted assets were expected to continue to face emergency food insecurity ~~though~~~~through~~ May  
807 2019 ~~characterized by large food consumption gaps reflected in acute malnutrition or are employing~~  
808 ~~emergency coping strategies.~~

## 809 5. Data Availability

810 The Central Asia data described in this manuscript can be accessed at the NASA GES DISC  
811 repository under data doi 10.5067/VQ4CD3Y9YC0R. The data citation is the following:

812 <sup>▲</sup> Jacob, Jossy and Slinski, Kimberly (NASA/GSFC/HSL) ~~(2021)~~~~(2021)~~, FLDAS Noah Land Surface  
813 Model L4 Central Asia Daily 0.01 x 0.01 degree, Greenbelt, MD, USA, Goddard Earth Sciences  
814 Data and Information Services Center (GES DISC), ~~Accessed: [Data Access Date].~~  
815 ~~10.5067/VQ4CD3Y9YC0R~~

816 <sup>▲</sup> The ~~Global~~~~global~~ data described in this manuscript can be accessed at the NASA GES DISC  
817 repository under data doi 10.5067/5NHC22T9375G. The data citation is the following:  
818

819 McNally, Amy. NASA/GSFC/HSL (2018), FLDAS Noah Land Surface Model L4 Global Monthly  
820 0.1 x 0.1 degree (MERRA-2 and CHIRPS), Greenbelt, MD, USA, Goddard Earth Sciences Data and  
821 Information Services Center (GES DISC), ~~Accessed: [Data Access Date].~~ 10.5067/5NHC22T9375G  
822

823 Currently the USGS EROS Center provides images from these data:  
824 <https://earlywarning.usgs.gov/fews/search/Asia/Central%20Asia>, as well as an interactive data  
825 viewer, the USGS ~~Early Warning eXplorer (EWX)~~ ~~https://earlywarning.usgs.gov/fews/software-~~  
826 ~~tools/1 (Shukla et al. 2021).~~ EWX (<https://earlywarning.usgs.gov/fews/ewx/>).

## 829 6. Code availability

830 The NASA Land Information System Framework (LISF) is publicly available and an open-source  
831 software. The software and technical support are available at <https://github.com/NASA-LIS/LISF>.

## 832 7. Conclusion

833 This paper describes a comprehensive hydrologic analysis system for food security monitoring in  
834 Central Asia, with analysis focusing on Afghanistan. ~~While these data are tailored to specific needs,~~  
835 ~~they are also applicable to other climate services and research.~~ Our intent is to provide the reader  
836 with ~~substantial~~ information regarding the configuration and specification of both the current global

Formatted: Font color: Auto

Formatted: Font color: Auto

Formatted: Font color: Auto

Formatted: Font color: Auto

Formatted: Font color: Auto

Formatted: Font color: Auto

Formatted: Font color: Auto

Formatted: Font color: Auto

Formatted: Font color: Auto

837 and Central Asia data streams. These data are publicly available and available at near-real time for  
838 food security decision support. ~~An important note is~~Note that, as an on-going initiative, FLDAS  
839 model version and parameters are routinely updated, and the user should consult the version updates  
840 provided by the NASA [Goddard Earth Science Data and Information Services Center \(GES DISC\)](#)  
841 data provider and documentation on USGS Early Warning website. For example, efforts are  
842 currently underway to upgrade to the Noah ~~with multi-parameterizations (Noah-MP)~~ (Niu et al.,  
843 2011)(Niu et al., 2011) land surface model, which requires some changes in parameters for snow,  
844 glaciers and groundwater. This, and future changes ~~will, can~~ be informed by the strengths and  
845 weaknesses of the data stream configurations that we have discussed in this paper.

846  
847 This paper also provides model-model and model-remote sensing comparisons, as well as a review  
848 of other research that highlights the challenges of quantitative evaluation of models and remote  
849 sensing in this region. A key challenge to hydrologic modeling is the considerable uncertainty in the  
850 meteorological forcing ~~available for this region,~~ particularly precipitation, ~~available for this region.~~  
851 Advancements in remote sensing and modeling should help reduce these uncertainties. In addition,  
852 the current land surface modeling ~~and river-routing frameworks reflect~~reflects natural conditions,  
853 i.e., they do not include representation of anthropogenic ~~impacts~~effects such as human water  
854 abstractions (e.g., dams for flood control or irrigation, water diversions, groundwater pumping,  
855 ~~etc.))~~ or land application of abstracted water (i.e., irrigation). These factors ~~impact streamflow~~  
856 ~~(through abstraction and irrigation flows) as well as~~affect estimates of ~~runoff,~~ soil moisture,  
857 evapotranspiration, and sensible heat flux (land surface temperatures) in irrigated areas. Therefore, it  
858 is important to be aware of the limitations and combine with other products (e.g., ~~Normalized~~  
859 ~~Difference-Vegetation-Index (NDVI)~~NDVI or Actual Evapotranspiration (ETa) in irrigated areas)  
860 when exploring water and energy balance. Even with improvements to meteorological forcing and  
861 modeling parameterizations, errors will remain. Therefore, the ‘convergence of evidence’ approach  
862 ~~that we advocate for here will continue to~~be beneficial and ~~would~~ be important when assessing  
863 hydro-meteorological hazards and associated risks to food and water security. ~~We hope that by~~By  
864 making the data publicly available the broader food security and water resources communities will  
865 be able to provide insights that ~~will~~can lead to improvements in our understanding of the water and  
866 energy balance that ~~will~~can ultimately lead to improvements to food and water security decision  
867 support systems.

## 869 8. Author contribution

870 JJ runs the code, updates websites, and archives routinely. DS maintains ~~LISLISF~~ code used in  
871 paper, JJ, KA, DS, SP conducted model evaluation AM, KS, CPL, SK contributed to design of  
872 evaluation. JR, MB, SP manage the data for USGS distribution. AH, JV ~~provides~~provide feedback  
873 on data quality and ~~interpretation~~interpretation. AM prepared the manuscript with contributions from  
874 all co-authors.



875 **9. Acknowledgements**

876 The authors wish to acknowledge the original version of the Central Asia snow modeling with LIS6  
877 performed at NOAA National Operational Hydrologic Remote Sensing Center by Greg Fall and  
878 Logan Karsten. USGS work was performed under [U.S. Agency for International Development](#)  
879 [\(USAID\), Bureau of Humanitarian Assistance \(BHA\) PAPA AID-FFP-T-17-00003](#) and USGS  
880 contract 140G0119C0001. Any use of trade, firm, or product names is for descriptive purposes only  
881 and does not imply endorsement by the U.S. Government. KS, AH, DS, JJ, NASA work was  
882 performed under [U.S. Agency for International Development, Bureau of Humanitarian](#)  
883 [Assistance USAID BHA PAPA AID-FFP-T-17-00001](#). KS, AH acknowledge support from the  
884 NASA Harvest Consortium (NASA Applied Sciences Grant No. 80NSSC17K0625). Computing  
885 resources have been provided by NASA's Center for Climate Simulation (NCCS). Distribution of  
886 data from the Goddard Earth Sciences Data and Information Services Center (GES DISC) is funded  
887 by NASA's Science Mission Directorate (SMD). We thank NOAA CPC International Desk for use  
888 of [Figures, The figures, and the](#) NASA Land Information System Team for software support and  
889 development. The authors also thank the USGS reviewer for comments that improved the quality of  
890 the manuscript.

891 **10. References**

- 892 Arsenault, K. R., Houser, P. R., and De Lannoy, G. J. M.: Evaluation of the MODIS snow cover  
893 fraction product: Satellite-based snow cover fraction evaluation., *Hydrol. Process.*, 28, 980–998,  
894 <https://doi.org/10.1002/hyp.9636>, 2014.
- 895 Arsenault, K. R., Kumar, S. V., Geiger, J. V., Wang, S., Kemp, E., Mocko, D. M., Beaudoin, H.  
896 K., Getirana, A., Navari, M., Li, B., Jacob, J., Wegiel, J., and Peters-Lidard, C. D.: The Land  
897 [surface](#) ~~Surface~~ Data Toolkit (LDT v7.2) — ~~a data fusion environment-~~ [A Data Fusion Environment](#)  
898 [for land data assimilation systems,](#) *Land Data Assimilation Systems. Geosci. Model Dev.*, 11, 3605–  
899 [3621](#), <https://doi.org/10.5194/gmd-11-3605-2018>, 2018.
- 900 [Barlage, M., Zeng, X., Wei, H., and Mitchell, K. E.: A global 0.05° maximum albedo dataset of](#)  
901 [snow-covered land based on MODIS observations: Maximum Albedo of Snow-covered,](#) *Geophys.*  
902 [Res. Lett.](#), 32, <https://doi.org/10.1029/2005GL022881>, 2005.
- 903 Barlow, M., Wheeler, M., Lyon, B., and Cullen, H.: Modulation of Daily Precipitation over  
904 Southwest Asia by the Madden–Julian Oscillation, *Monthly Weather Review*, 133, 3579–3594,  
905 <https://doi.org/10.1175/MWR3026.1>, 2005.
- 906 Barlow, M., Zaitchik, B., Paz, S., Black, E., Evans, J., and Hoell, A.: A Review of Drought in the  
907 Middle East and Southwest Asia, *Journal of Climate*, 29, 8547–8574, <https://doi.org/10.1175/JCLI->  
908 [D-13-00692.1](#), 2016.

Formatted: Font color: Auto

Formatted: Font color: Auto

Formatted: Font color: Auto

Formatted: Font color: Auto

Formatted: Font color: Auto

909 Carroll, M., DiMiceli, C., Wooten, M., Hubbard, A., Sohlberg, R., and Townshend, J.: MOD44W  
910 MODIS/Terra Land Water Mask Derived from MODIS and SRTM L3 Global 250m SIN Grid V006  
911 [Data set]. NASA EOSDIS Land Processes DAAC., [NASA EOSDIS Land Processes DAAC.](#),  
912 [NASA EOSDIS Land Processes DAAC.](#), 2017.

913 Chen, F., Mitchell, K., Schaake, J., Xue, Y., Pan, H.-L., Koren, V., Duan, Q. Y., Ek, M., and Betts,  
914 A.: Modeling of land surface evaporation by four schemes and comparison with FIFE observations,  
915 *J. Geophys. Res.*, 101, 7251–7268, <https://doi.org/10.1029/95JD02165>, 1996.

916 CIA World Factbook: <https://www.cia.gov/the-world-factbook/countries/afghanistan/#introduction>.

917 Cosgrove, B. A., Lohmann, D., Mitchell, K. E., Houser, P. R., Wood, E. F., Schaake, J. C., Robock,  
918 A., Marshall, C., Sheffield, J., Duan, Q., Luo, L., Higgins, R. W., Pinker, R. T., Tarpley, J. D., and  
919 Meng, J.: Real-time and retrospective forcing in the North American Land Data Assimilation  
920 System (NLDAS) project, *J. Geophys. Res.*, 108, 2002JD003118,  
921 <https://doi.org/10.1029/2002JD003118>, 2003.

922 CPC NOAA: Weather Hazards Outlook of Afghanistan and Central Asia for the Period of February  
923 22 - 28, 2018, 2018.

924 [Csiszar, I. and Gutman, G.: Mapping global land surface albedo from NOAA AVHRR, 104, 6215–](#)  
925 [6228, <https://doi.org/10.1029/1998JD200090>, 1999.](#)

926 Davenport, F. M., Harrison, L., Shukla, S., Husak, G., Funk, C., and McNally, A.: Using out-of-  
927 sample yield forecast experiments to evaluate which earth observation products best indicate end of  
928 season maize yields, *Environ. Res. Lett.*, 14, 124095, <https://doi.org/10.1088/1748-9326/ab5ccd>,  
929 2019.

930 Derber, J. C., Parrish, D. F., and Lord, S. J.: The New Global Operational Analysis System at the  
931 National Meteorological Center, [Weather and Forecasting](#), 6, 538–547,  
932 [https://doi.org/10.1175/1520-0434\(1991\)006<0538:TNGOAS>2.0.CO;2](https://doi.org/10.1175/1520-0434(1991)006<0538:TNGOAS>2.0.CO;2), 1991.

933 Dezfuli, A. K., Ichoku, C. M., Huffman, G. J., Mohr, K. I., Selker, J. S., van de Giesen, N.,  
934 Hochreutener, R., and Annor, F. O.: Validation of IMERG Precipitation in Africa, [Journal of](#)  
935 [Hydrometeorology](#), 18, 2817–2825, <https://doi.org/10.1175/JHM-D-17-0139.1>, 2017.

936 Ek, M. B., Mitchell, K. E., Lin, Y., Rogers, E., Grunmann, P., Koren, V., Gayno, G., and Tarpley, J.  
937 D.: Implementation of Noah land surface model advances in the National Centers for Environmental  
938 Prediction operational mesoscale Eta model, [JGR: Atmospheres](#), 108,  
939 <https://doi.org/10.1029/2002JD003296>, 2003.

940 [Fall, G.: NOAA National Operational Hydrologic Remote Sensing Center, 2014.](#)

941 [Ellenburg, W. L., Mishra, V., Roberts, J. B., Limaye, A. S., Case, J. L., Blankenship, C. B., and](#)  
942 [Cressman, K.: Detecting Desert Locust Breeding Grounds: A Satellite-Assisted Modeling](#)  
943 [Approach, Remote Sensing, 13, 1276, <https://doi.org/10.3390/rs13071276>, 2021.](#)

944 [Entekhabi, D., Njoku, E. G., O'Neill, P. E., Kellogg, K. H., Crow, W. T., Edelstein, W. N., Entin, J.](#)  
945 [K., Goodman, S. D., Jackson, T. J., Johnson, J., Kimball, J., Piepmeier, J. R., Koster, R. D., Martin,](#)  
946 [N., McDonald, K. C., Moghaddam, M., Moran, S., Reichle, R., Shi, J. C., Spencer, M. W.,](#)  
947 [Thurman, S. W., Tsang, L., and Zyl, J. V.: The Soil Moisture Active Passive \(SMAP\) Mission, 98,](#)  
948 [704–716, <https://doi.org/10.1109/JPROC.2010.2043918>, 2010.](#)

949 [Entekhabi, D., Das, N., Njoku, E. G., Johnson, J., and Shi, J. C.: SMAP L3 Radar/Radiometer](#)  
950 [Global Daily 9 km EASE-Grid Soil Moisture, Version 3, NASA National Snow and Ice Data Center](#)  
951 [DAAC \[preprint\], <https://doi.org/10.5067/7KKNQ5UURM2W>, 2016.](#)

952 FEWS NET: Afghanistan Food Security Outlook October 2017-May 2018 Conflict, dry spells, and  
953 weak labor opportunities will lead to deterioration in outcomes during 2018 lean season, 2017a.

954 FEWS NET: Update on performance of the October 2016 – May 2017 wet season, 2017b.

955 FEWS NET: Afghanistan Food Security Outlook: Emergency assistance needs are atypically high  
956 through the lean season across the country, FEWS NET, 2018a.

957 FEWS NET: Afghanistan Food Security Outlook February to September 2018: Low snow  
958 accumulation and dry soil conditions likely to impact 2018 staple production, 2018b.

959 FEWS NET: Afghanistan Food Security Outlook Update April 2018: Poor rangeland conditions and  
960 below-average water availability will limit seasonal improvements, 2018c.

961 FEWS NET: El Niño and Precipitation, FEWS NET, [https://fews.net/el-ni%C3%B1o-and-](https://fews.net/el-ni%C3%B1o-and-precipitation)  
962 [precipitation](https://fews.net/el-ni%C3%B1o-and-precipitation), 2020a.

963 FEWS NET: La Niña and Precipitation, FEWS NET, [https://fews.net/la-ni%C3%B1a-and-](https://fews.net/la-ni%C3%B1a-and-precipitation)  
964 [precipitation](https://fews.net/la-ni%C3%B1a-and-precipitation), 2020b.

965 FEWS NET: Afghanistan Food Security Outlook February to September 2021: Below-average  
966 precipitation likely to drive below-average agricultural and livestock production in 2021, 2021.

967 Funk, C., Peterson, P., Landsfeld, M., Pedreros, D., Verdin, J., Shukla, S., Husak, G., Rowland, J.,  
968 Harrison, L., Hoell, A., and Michaelsen, J.: The climate hazards infrared precipitation with stations--  
969 a new environmental record for monitoring extremes., The climate hazards infrared precipitation  
970 with stations—a new environmental record for monitoring extremes, Sci Data, 2, 2, 150066–  
971 150066, <https://doi.org/10.1038/sdata.2015.66>, 10.1038/sdata.2015.66, 2015.

972 [Funk, C. C., Peterson, P., Huffman, G. J., Landsfeld, M. F., Peters-Lidard, C., Davenport, F.,](#)  
973 [Shukla, S., Peterson, S., Pedreros, D. H., Ruane, A. C., Mutter, C., Turner, W., Harrison, L.,](#)  
974 [Sonnier, A., Way-Henthorne, J., and Husak, G. J.: Introducing and Evaluating the Climate Hazards](#)  
975 [Center IMERG with Stations \(CHIMES\): Timely Station-Enhanced Integrated Multisatellite](#)  
976 [Retrievals for Global Precipitation Measurement, 103, E429–E454, \[https://doi.org/10.1175/BAMS-\]\(https://doi.org/10.1175/BAMS-D-20-0245.1\)](#)  
977 [D-20-0245.1, 2022.](#)

978 Gadelha, A. N., Coelho, V. H. R., Xavier, A. C., Barbosa, L. R., Melo, D. C. D., Xuan, Y.,  
979 Huffman, G. J., Petersen, W. A., and Almeida, C. das N.: Grid box-level evaluation of IMERG over  
980 Brazil at various space and time scales, *Atmospheric Research*, 218, 231–244,  
981 <https://doi.org/10.1016/j.atmosres.2018.12.001>, 2019.

982 Gelaro, R., McCarty, W., Suárez, M. J., Todling, R., Molod, A., Takacs, L., Randles, C. A.,  
983 Darmenov, A., Bosilovich, M. G., Reichle, R., Wargan, K., Coy, L., Cullather, R., Draper, C.,  
984 Akella, S., Buchard, V., Conaty, A., da Silva, A. M., Gu, W., Kim, G.-K., Koster, R., Lucchesi, R.,  
985 Merkova, D., Nielsen, J. E., Partyka, G., Pawson, S., Putman, W., Rienecker, M., Schubert, S. D.,  
986 Sienkiewicz, M., and Zhao, B.: The Modern-Era Retrospective Analysis for Research and  
987 Applications, Version 2 (MERRA-2), *J. Climate*, 30, 5419–5454, [https://doi.org/10.1175/JCLI-D-](https://doi.org/10.1175/JCLI-D-16-0758.1)  
988 [16-0758.1](#), 2017.

989 GEOGLAM: Early Warning Crop Monitor February 2018,  
990 [https://cropmonitor.org/documents/EWCM/reports/EarlyWarning\\_CropMonitor\\_201802.pdf](https://cropmonitor.org/documents/EWCM/reports/EarlyWarning_CropMonitor_201802.pdf),  
991 2018a.

992 GEOGLAM: Early Warning Crop Monitor March 2018,  
993 [https://cropmonitor.org/documents/EWCM/reports/EarlyWarning\\_CropMonitor\\_201802.pdf](https://cropmonitor.org/documents/EWCM/reports/EarlyWarning_CropMonitor_201802.pdf),  
994 2018b.

995 Ghatak, D., Zaitchik, B., Kumar, S., Matin, M. A., Bajracharya, B., Hain, C., and Anderson, M.:  
996 Influence of Precipitation Forcing Uncertainty on Hydrological Simulations with the NASA South  
997 Asia Land Data Assimilation System, *Hydrology*, 5, 57, <https://doi.org/10.3390/hydrology5040057>,  
998 2018.

999 Grace, K. and Davenport, F.: Climate variability and health in extremely vulnerable communities:  
1000 investigating variations in surface water conditions and food security in the West African Sahel,  
1001 *Population & Environment*, 42, 553–577, <https://doi.org/10.1007/s11111-021-00375-9>, 2021.

1002 [Gutman, G. and Ignatov, A.: The derivation of the green vegetation fraction from NOAA/AVHRR](#)  
1003 [data for use in numerical weather prediction models, \*International Journal of Remote Sensing\*, 19,](#)  
1004 [1533–1543, <https://doi.org/10.1080/014311698215333>, 1998.](#)

1005 Hall, D. and Riggs, G.: MODIS/Terra Snow Cover Daily L3 Global 500m SIN Grid [version 6](#),  
1006 <https://doi.org/10.5067/MODIS/MOD10A1.006>, 2016.

1007 [Hengl, T., Jesus, J. M. de, Heuvelink, G. B. M., Gonzalez, M. R., Kilibarda, M., Blagotić, A.,](#)  
1008 [Shangguan, W., Wright, M. N., Geng, X., Bauer-Marschallinger, B., Guevara, M. A., Vargas, R.,](#)  
1009 [MacMillan, R. A., Batjes, N. H., Leenaars, J. G. B., Ribeiro, E., Wheeler, I., Mantel, S., and](#)  
1010 [Kempen, B.: SoilGrids250m: Global gridded soil information based on machine learning, PLOS](#)  
1011 [ONE, 12, e0169748, <https://doi.org/10.1371/journal.pone.0169748>, 2017.](#)

1012 [Hewitt, C., Mason, S., and Walland, D.: The Global Framework for Climate Services, Nature Clim](#)  
1013 [Change, 2, 831–832, <https://doi.org/10.1038/nclimate1745>, 2012.](#)

1014 Hoell, A., Funk, C., and Barlow, M.: The Forcing of Southwestern Asia Teleconnections by Low-  
1015 Frequency Sea Surface Temperature Variability during Boreal Winter, [J. Climate](#), 28, 1511–1526,  
1016 <https://doi.org/10.1175/JCLI-D-14-00344.1>, 2015.

1017 Hoell, A., Barlow, M., Cannon, F., and Xu, T.: Oceanic Origins of Historical Southwest Asia  
1018 Precipitation During the Boreal Cold Season, [J. Climate](#), 30, 2885–2903,  
1019 <https://doi.org/10.1175/JCLI-D-16-0519.1>, 2017.

1020 Hoell, A., Cannon, F., and Barlow, M.: Middle East and Southwest Asia Daily Precipitation  
1021 Characteristics Associated with the Madden–Julian Oscillation during Boreal Winter, [J. Climate](#), 31,  
1022 8843–8860, <https://doi.org/10.1175/JCLI-D-18-0059.1>, 2018.

1023 Hoell, A., Eischeid, J., Barlow, M., and McNally, A.: Characteristics, precursors, and potential  
1024 predictability of Amu Darya Drought in an Earth system model large ensemble, [Clim Dyn](#), 55,  
1025 2185–2206, <https://doi.org/10.1007/s00382-020-05381-5>, 2020.

1026 Huffman, G. J., Bolvin, D. T., Braithwaite, D., Hsu, K.-L., Joyce, R. J., Kidd, C., Nelkin, E. J.,  
1027 Sorooshian, S., Stocker, E. F., Tan, J., Wolff, D. B., and Xie, P.: Integrated Multi-satellite Retrievals  
1028 for the Global Precipitation Measurement (GPM) Mission (IMERG), in: [Satellite Precipitation](#)  
1029 [Measurement: Volume 1](#), edited by: Levizzani, V., Kidd, C., Kirschbaum, D. B., Kummerow, C. D.,  
1030 Nakamura, K., and Turk, F. J., Springer International Publishing, Cham, 343–353,  
1031 [https://doi.org/10.1007/978-3-030-24568-9\\_19](https://doi.org/10.1007/978-3-030-24568-9_19), 2020.

1032 Immerzeel, W. W., Wanders, N., Lutz, A. F., Shea, J. M., and Bierkens, M. F. P.: Reconciling high-  
1033 altitude precipitation in the upper Indus basin with glacier mass balances and runoff, [Hydrol. Earth](#)  
1034 [Syst. Sci.](#), 19, 4673–4687, <https://doi.org/10.5194/hess-19-4673-2015>, 2015.

1035 Jacob, J. and Sliniski, K.: GES DISC Dataset: FLDAS Noah Land Surface Model L4 Central Asia  
1036 Daily 0.01 x 0.01 degree (FLDAS\_NOAH001\_G\_CA\_D 001),  
1037 [2021-<https://doi.org/10.5067/VQ4CD3Y9YC0R>, 2021.](https://doi.org/10.5067/VQ4CD3Y9YC0R)

1038 Jung, H. C., Getirana, A., Policelli, F., McNally, A., Arsenault, K. R., Kumar, S., Tadesse, T., and  
1039 Peters-Lidard, C. D.: Upper Blue Nile basin water budget from a multi-model perspective, [Journal](#)  
1040 [of Hydrology](#), 555, 535–546, <https://doi.org/10.1016/j.jhydrol.2017.10.040>, 2017.

1041 Jung, H. C., Getirana, A., Arsenault, K. R., Holmes, T. R. H., and McNally, A.: Uncertainties in  
1042 Evapotranspiration Estimates over West Africa, [Remote Sensing](#), 11, 892,  
1043 <https://doi.org/10.3390/rs11080892>, 2019.

1044 [Kato, H. and Rodell, M.: Sensitivity of Land Surface Simulations to Model Physics, Land](#)  
1045 [Characteristics, and Forcings, at Four CEOP Sites, Journal of the Meteorological Society of Japan,](#)  
1046 [Ser. II, Volume 85A, 187–204, https://doi.org/10.2151/jmsj.85A.187, 2007.](#)

1047 Kirschbaum, D. B., Huffman, G. J., Adler, R. F., Braun, S., Garrett, K., Jones, E., McNally, A.,  
1048 Skofronick-Jackson, G., Stocker, E., Wu, H., and Zaitchik, B. F.: NASA’s Remotely Sensed  
1049 Precipitation: A Reservoir for Applications Users, *Bull. Amer. Meteor. Soc.*, 98, 1169–1184,  
1050 <https://doi.org/10.1175/BAMS-D-15-00296.1>, 2016.

1051 Kumar, S. V., Peters-Lidard, C. D., Tian, Y., Houser, P. R., Geiger, J., Olden, S., Lighty, L.,  
1052 Eastman, J. L., Doty, B., Dirmeyer, P., Adams, J., Mitchell, K., Wood, E. F., and Sheffield, J.: Land  
1053 information system: An interoperable framework for high resolution land surface modeling,  
1054 *Environmental Modelling & Software*, 21, 1402–1415,  
1055 <https://doi.org/10.1016/j.envsoft.2005.07.004>, 2006.

1056 Kumar, S. V., Peters-Lidard, C. D., Santanello, J., Harrison, K., Liu, Y., and Shaw, M.: Land  
1057 surface Verification Toolkit (LVT) – a generalized framework for land surface model evaluation,  
1058 *Geosci. Model Dev.*, 5, 869–886, <https://doi.org/10.5194/gmd-5-869-2012>, 2012.

1059 Kumar, S. V., Peters-Lidard, C. D., Mocko, D., and Tian, Y.: Multiscale Evaluation of the  
1060 Improvements in Surface Snow Simulation through Terrain Adjustments to Radiation, [Journal of](#)  
1061 [Hydrometeorology](#), 14, 220–232, <https://doi.org/10.1175/JHM-D-12-046.1>, 2013.

1062 Ma, Z., Xu, J., Zhu, S., Yang, J., Tang, G., Yang, Y., Shi, Z., and Hong, Y.: AIMERG: a new Asian  
1063 precipitation dataset (0.1°/half-hourly, 2000–2015) by calibrating the GPM-era IMERG at a daily  
1064 scale using APHRODITE, [Earth Syst. Sci. Data](#), 12, 1525–1544, [https://doi.org/10.5194/essd-12-](https://doi.org/10.5194/essd-12-1525-2020)  
1065 [1525-2020](https://doi.org/10.5194/essd-12-1525-2020), 2020.

1066 Manz, B., Páez-Bimos, S., Horna, N., Buytaert, W., Ochoa-Tocachi, B., Lavado-Casimiro, W., and  
1067 Willems, B.: Comparative Ground Validation of IMERG and TMPA at Variable Spatiotemporal  
1068 Scales in the Tropical Andes, [Journal of Hydrometeorology](#), 18, 2469–2489,  
1069 <https://doi.org/10.1175/JHM-D-16-0277.1>, 2017.

1070 McNally, A.: GES DISC Dataset: FLDAS Noah Land Surface Model L4 Global Monthly 0.1 x 0.1  
1071 degree (MERRA-2 and CHIRPS) (FLDAS\_NOAH01\_C\_GL\_M 001), 2018.

1072 McNally, A., Husak, G. J., Brown, M., Carroll, M., Funk, C., Yatheendradas, S., Arsenault, K.,  
1073 Peters-Lidard, C., and Verdin, J. P.: Calculating Crop Water Requirement Satisfaction in the West

1074 Africa Sahel with Remotely Sensed Soil Moisture, *J. Hydrometeor.*, 16, 295–305,  
1075 <https://doi.org/10.1175/JHM-D-14-0049.1>, 2015.

1076 McNally, A., Shukla, S., Arsenault, K. R., Wang, S., Peters-Lidard, C. D., and Verdin, J. P.:  
1077 Evaluating ESA CCI soil moisture in East Africa, *International Journal of Applied Earth*  
1078 *Observation and Geoinformation*, 48, 96–109, <https://doi.org/10.1016/j.jag.2016.01.001>, 2016.

1079 McNally, A., Arsenault, K., Kumar, S., Shukla, S., Peterson, P., Wang, S., Funk, C., Peters-lidard,  
1080 C. D., and Verdin, J. P.: A land data assimilation system for sub-Saharan Africa food and water  
1081 security applications, *Scientific Data*, 4, 170012, <http://dx.doi.org/10.1038/sdata.2017.12>, 2017.

1082 McNally, A., McCartney, S., Ruane, A. C., Mladenova, I. E., Whitcraft, A. K., Becker-Reshef, I.,  
1083 Bolten, J. D., Peters-Lidard, C. D., Rosenzweig, C., and Uz, S. S.: Hydrologic and Agricultural  
1084 Earth Observations and Modeling for the Water-Food Nexus, *Front. Environ. Sci.*, 7,  
1085 <https://doi.org/10.3389/fenvs.2019.00023>, 2019.

1086 [Miller, J., Barlage, M., Zeng, X., Wei, H., Mitchell, K., and Tarpley, D.: Sensitivity of the](#)  
1087 [NCEP/Noah land surface model to the MODIS green vegetation fraction data set, \*Geophys. Res.\*](#)  
1088 [\*Lett.\*, 33, <https://doi.org/10.1029/2006GL026636>, 2006.](#)

1089 [Molteni, F., Buizza, R., Palmer, T. N., and Petroliagis, T.: The ECMWF Ensemble Prediction](#)  
1090 [System: Methodology and validation, \*Q J R Meteorol Soc.\*, 122, 73–119,](#)  
1091 <https://doi.org/10.1002/qj.49712252905>, 1996.

1092 [NASA Earth Observatory: Record Low Snowpack in Afghanistan:](#)  
1093 <https://earthobservatory.nasa.gov/images/91851/record-low-snowpack-in-afghanistan>, last access:  
1094 [20 March, NASA Earth Observatory, 2018.](#)

1095 NASA JPL: NASA Shuttle Radar Topography Mission Global 30 arc second [Data set]. NASA  
1096 EOSDIS Land Processes DAAC, NASA EOSDIS Land Processes DAAC, NASA EOSDIS Land  
1097 Processes DAAC., 2013.

1098 Nazemosadat, M. J. and Ghaedamini, H.: On the Relationships between the Madden–Julian  
1099 Oscillation and Precipitation Variability in Southern Iran and the Arabian Peninsula: Atmospheric  
1100 Circulation Analysis, 23, 887–904, <https://doi.org/10.1175/2009JCLI2141.1>, 2010.

1101 NCAR Research Applications Library: <https://ral.ucar.edu/solutions/products/unified-noah-lsm>, last  
1102 access: 12 November 2021.

1103 [Nguyen, P., Thorstensen, A., Sorooshian, S., Hsu, K., Aghakouchak, A., Ashouri, H., Tran, H., and](#)  
1104 [Braithwaite, D.: Global Precipitation Trends across Spatial Scales Using Satellite Observations, 99,](#)  
1105 [689–697, https://doi.org/10.1175/BAMS-D-17-0065.1](https://doi.org/10.1175/BAMS-D-17-0065.1), 2018.

1106 Niu, G.-Y., Yang, Z.-L., Mitchell, K. E., Chen, F., Ek, M. B., Barlage, M., Kumar, A., Manning, K.,  
1107 Niyogi, D., Rosero, E., Tewari, M., and Xia, Y.: The community Noah land surface model with  
1108 multiparameterization options (Noah-MP): 1. Model description and evaluation with local-scale  
1109 measurements, *JGR: Atmospheres*, 116, <https://doi.org/10.1029/2010JD015139>, 2011.

1110 NOAA: [https://www.climate.gov/news-features/blogs/enso/september-enso-update-la-ni%C3%B1a-](https://www.climate.gov/news-features/blogs/enso/september-enso-update-la-ni%C3%B1a-watch)  
1111 watch, last access: 12 September 2017.

1112 NOAA CPC ENSO Cold & Warm Episodes by Season:  
1113 [https://origin.cpc.ncep.noaa.gov/products/analysis\\_monitoring/ensostuff/ONI\\_v5.php](https://origin.cpc.ncep.noaa.gov/products/analysis_monitoring/ensostuff/ONI_v5.php), last access:  
1114 29 July 2021.

1115 Oki, T. and Kanae, S.: Global Hydrological Cycles and World Water Resources, *Science*, 313,  
1116 1068–1072, <https://doi.org/10.1126/science.1128845>, 2006.

1117 Pervez, S., McNally, A., Arsenault, K., Budde, M., and Rowland, J.: Vegetation Monitoring  
1118 Optimization With Normalized Difference Vegetation Index and Evapotranspiration Using Remote  
1119 Sensing Measurements and Land Surface Models Over East Africa, *Frontiers in Climate*, 3, 1,  
1120 <https://doi.org/10.3389/fclim.2021.589981>, 2021.

1121 Peters-Lidard, C. D., Houser, P. R., Tian, Y., Kumar, S. V., Geiger, J., Olden, S., Lighty, L., Doty,  
1122 B., Dirmeyer, P., Adams, J., Mitchell, K., Wood, E. F., and Sheffield, J.: High-performance Earth  
1123 system modeling with NASA/GSFC's Land Information System, *Innovations Syst Softw Eng*, 3,  
1124 157–165, <https://doi.org/10.1007/s11334-007-0028-x>, 2007.

1125 Qamer, F. M., Tadesse, T., Matin, M., Ellenburg, W. L., and Zaitchik, B.: Earth Observation and  
1126 Climate Services for Food Security and Agricultural Decision Making in South and Southeast Asia,  
1127 *Bull Am Meteorol Soc*, 100, ES171–ES174, <https://doi.org/10.1175/BAMS-D-18-0342.1>, 2019.

1128 Rana, S., Renwick, J., McGregor, J., and Singh, A.: Seasonal Prediction of Winter Precipitation  
1129 Anomalies over Central Southwest Asia: A Canonical Correlation Analysis Approach, *J. Climate*,  
1130 31, 727–741, <https://doi.org/10.1175/JCLI-D-17-0131.1>, 2018.

1131 Rodell, M., Famiglietti, J. S., Wiese, D. N., Reager, J. T., Beaudoing, H. K., Landerer, F. W., and  
1132 Lo, M.-H.: Emerging trends in global freshwater availability, 557, 651,  
1133 <https://doi.org/10.1038/s41586-018-0123-1>, 2018.

1134 Reynolds, C. A., Jackson, T. J., and Rawls, W. J.: Estimating soil water-holding capacities by  
1135 linking the Food and Agriculture Organization Soil map of the world with global pedon databases  
1136 and continuous pedotransfer functions, *Water Resources Research*, 36, 3653–3662,  
1137 <https://doi.org/10.1029/2000WR900130>, 2000.



1138 Sarmiento, D. P., Slinski, K., McNally, A., Funk, C., Peterson, P., and Peters-Lidard, C. D.: Daily  
1139 precipitation frequency distributions impacts on land-surface simulations of CONUS, *Front. Water*,  
1140 0, <https://doi.org/10.3389/frwa.2021.640736>, 2021.

1141 Schiemann, R., Lüthi, D., Vidale, P. L., and Schär, C.: The precipitation climate of Central Asia—  
1142 intercomparison of observational and numerical data sources in a remote semiarid region, *Royal*  
1143 *Meteorological Society*, 28, 295–314, <https://doi.org/10.1002/joc.1532>, 2008.

1144 Schneider, U., Finger, P., Meyer-Christoffer, A., Rustemeier, E., Ziese, M., and Becker, A.:  
1145 [Evaluating the Hydrological Cycle over Land Using the Newly-Corrected Precipitation Climatology](https://doi.org/10.3390/atmos8030052)  
1146 [from the Global Precipitation Climatology Centre \(GPCC\)](https://doi.org/10.3390/atmos8030052), 8, 52,  
1147 <https://doi.org/10.3390/atmos8030052>, 2017.

1148 Senay, G. B., Bohms, S., Singh, R. K., Gowda, P. H., Velpuri, N. M., Alemu, H., and Verdin, J. P.:  
1149 [Operational Evapotranspiration Mapping Using Remote Sensing and Weather Datasets: A New](https://doi.org/10.1111/jawr.12057)  
1150 [Parameterization for the SSEB Approach](https://doi.org/10.1111/jawr.12057), *J Am Water Resour Assoc.* 49, 577–591,  
1151 <https://doi.org/10.1111/jawr.12057>, 2013.

1152 Shukla, S., Arsenault, K. R., Hazra, A., Peters-Lidard, C., Koster, R. D., Davenport, F., Magadzire,  
1153 T., Funk, C., Kumar, S., McNally, A., Getirana, A., Husak, G., Zaitchik, B., Verdin, J., Nsadisa, F.  
1154 D., and Becker-Reshef, I.: Improving early warning of drought-driven food insecurity in southern  
1155 Africa using operational hydrological monitoring and forecasting products, *Nat. Hazards Earth Syst.*  
1156 *Sci.*, 20, 1187–1201, <https://doi.org/10.5194/nhess-20-1187-2020>, 2020.

1157 Shukla, S., Landsfeld, M., Anthony, M., Budde, M., Husak, G. J., Rowland, J., and Funk, C.:  
1158 Enhancing the Application of Earth Observations for Improved Environmental Decision-Making  
1159 Using the Early Warning eXplorer (EWX), *Frontiers in Climate*, 2, 34,  
1160 <https://doi.org/10.3389/fclim.2020.583509>, 2021.

1161 Tabar, M., Gluck, J., Goyal, A., Jiang, F., Morr, D., Kehs, A., Lee, D., Hughes, D. P., and Yadav,  
1162 A.: [A PLAN for Tackling the Locust Crisis in East Africa: Harnessing Spatiotemporal Deep Models](https://doi.org/10.1145/3447548.3467184)  
1163 [for Locust Movement Forecasting](https://doi.org/10.1145/3447548.3467184), in: *Proceedings of the 27th ACM SIGKDD Conference on*  
1164 *Knowledge Discovery & Data Mining*, New York, NY, USA, 3595–3604,  
1165 <https://doi.org/10.1145/3447548.3467184>, 2021.

1166 Tan, J., Petersen, W. A., and Tokay, A.: A Novel Approach to Identify Sources of Errors in IMERG  
1167 for GPM Ground Validation, *Journal of Hydrometeorology*, 17, 2477–2491,  
1168 <https://doi.org/10.1175/JHM-D-16-0079.1>, 2016.

1169 UNICEF: 500,000 children affected by drought in Afghanistan – UNICEF,  
1170 <https://www.unicef.org/press-releases/500000-children-affected-drought-afghanistan-unicef>, last  
1171 access: 23 April 2018.

1172 USGS [KnowledgeBase](#):  
1173 <https://earlywarning.usgs.gov/fews/searchkb/Asia/Central%20Asia/Afghanistan>, last access: 12  
1174 November 2021.

1175 [Verdin, A., Funk, C., Peterson, P., Landsfeld, Vincent, K., Daly, M., Tuholske, Scannell, C., and](#)  
1176 [Grace, K.; Leathes, B.: What can climate services learn from theory and](#)  
1177 [validation practice of the CHIRTS daily quasi-global high-resolution daily temperature data set, Sci](#)  
1178 [Data, 7, 303co-production?, Climate Services, 12, 48–58, https://doi.org/10.1038/s41597-020-](#)  
1179 [00643-7, 20201016/j.cliser.2018.11.001, 2018.](#)

1180 Xie, P. and Arkin, P. A.: Analyses of Global Monthly Precipitation Using Gauge Observations,  
1181 Satellite Estimates, and Numerical Model Predictions, [Journal of Climate](#), 9, 840–858,  
1182 [https://doi.org/10.1175/1520-0442\(1996\)009<0840:AOGMPU>2.0.CO;2](https://doi.org/10.1175/1520-0442(1996)009<0840:AOGMPU>2.0.CO;2), 1996.

1183 Yatagai, A., Kamiguchi, K., Arakawa, O., Hamada, A., Yasutomi, N., and Kitoh, A.: APHRODITE:  
1184 Constructing a Long-Term Daily Gridded Precipitation Dataset for Asia Based on a Dense Network  
1185 of Rain Gauges, [Bull Am Meteorol Soc](#), 93, 1401–1415, <https://doi.org/10.1175/BAMS-D-11->  
1186 [00122.1](#), 2012.

1187 Yoon, Y., Kumar, S. V., Forman, B. A., Zaitchik, B. F., Kwon, Y., Qian, Y., Rupper, S., Maggioni,  
1188 V., Houser, P., Kirschbaum, D., Richey, A., Arendt, A., Mocko, D., Jacob, J., Bhanja, S., and  
1189 Mukherjee, A.: Evaluating the Uncertainty of Terrestrial Water Budget Components Over High  
1190 Mountain Asia, [Frontiers in Earth Science](#), 7, 120, <https://doi.org/10.3389/feart.2019.00120>, 2019.

1191